



H2020-ICT-25-2016-2017



HYbrid FLying rollIng with-snake-aRm robot for contact inSpection

HYFLIERS

D2.1

Design of the hybrid robot

Contractual date of delivery	30-June-2019
Actual date of delivery	30-June-2019
Editor(s)	Guillermo Heredia (USE)
Author(s)	P.J. Sanchez-Cuevas (USE), P. Grau (USE), F. Alarcon (CATEC), R. Schmid (GEIR), V. Lippiello (CREATE), J. A. Acosta (USE), B. Arrue (USE), A. Viguria (CATEC) and A. Ollero (USE)
Workpackage	WP2
Estimated person-months	42
Dissemination level	PU
Type	R
Version	1.0
Total number of pages	69

Abstract:

This document is about the design and development of the versatile hybrid robots for contact inspection with application to pipe inspection. Two prototypes are presented to accomplish the inspection applications. These designs include the proposed architecture and the aerial platform details, as well as a description of the inspection devices and a short description of the UT sensor integration. Moreover, both are able to take-off, fly and land on a pipe.

Keywords:

Hybrid robot. Aerial robot. Satellite robot. Magnetic attractor. Hyper-redundant robotic arm. UT inspection. Miniature UT probe. Pipe inspection. Remote inspection. Refinery. Operations support. Ground station. Emergency behaviour.

Executive summary

This document describes the design of the hybrid robot prototypes developed in the HYFLIERS project. Based on the initial system specification (D1.1) and following the consideration of the system concept architecture (D1.2), two different prototypes are presented with different scope:

- Hybrid Mobile Robot (HMR):
 - using a satellite slave robot that moves from the lander to the inspection location on the pipe,
 - for landing on magnetic pipes,
 - inspection of single pipes or in racks,
 - minimum clearance between tubes 100mm,
 - inspection of the landing pipe only,
 - straight sections, elbows as far as possible;
- Hybrid Robot with Arm (HRA):
 - using a robotic arm and a robot base with movement capability for landing on magnetic and non-magnetic pipes,
 - modular concept which can work in isolated pipes or racks,
 - access to different pipes or structures from the landing pipe with a robotic arm,
 - for more complex tasks on larger pipes.

The design of both platforms presented in this deliverable includes details about the aerial platform, the different landing gears for the pipe inspection, the satellite robot (in HMR) and the robotic arm (in HRA). It is also presents how these systems can mount the UT sensors.

The global architecture of the HYFLIERS system and the specifications of each platform are also described.

Abbreviations and symbols

CAN	Controller Area Network
CATEC	Centro Avanzado de Tecnología Aeroespaciales
CMD	Command prompt
CoM	Centre of Mass
CREATE	Consorzio C.R.E.A.T.E.
DBUS	Desktop Bus
DC	Direct Current
DN	Diameter Nominal
DoF	Degree of Freedom
EC	European Commission
ETH	Ethernet
ESC	Electronic Speed Controller
FPV	First Person View
FRR	Full Requirement Robot
FuMo	Functional Model
GEIR	GE Inspection Robotics
GPS	Global Positioning System
HD	High Definition
HDMI	High Definition Multimedia Interface
HLC	High Level Computer
HYFLIERS	Hybrid flying rolling with-snake-arm robot for contact inspection
HMR	Hybrid Mobile Robot
HRA	Hybrid Robot w/ Arm
ICT	Information and communications technology
IMU	Inertial Measurement Unit
GCS	Ground Control Station
LCD	Liquid Crystal Display
LiPo	Lithium-Polymer
LRR	Limited Requirement Robot
PC	Personal Computer
PPM	Pulse-Position Modulation
PWM	Pulse Width Modulation
RGB	Red Green Blue
RPA	Remotely Piloted Aircraft
SAP	Snake Arm with pan and tilt Probe
TRL	Technology Readiness Level
TX	Transmitter
UAV	Unmanned Aerial Vehicle
USB	Universal Serial Bus
USE	Universidad de Sevilla

UT	Ultrasonic
VMC	Visual Meteorological Conditions
WP	Workpackage

Table of Contents

Executive summary	2
Abbreviations and symbols	3
1. Introduction	10
1.1. Basic Requirements	10
1.2. Design Approach	10
1.2.1. Approach 1 Overview: Hybrid Mobile Robot (HMR)	10
1.2.2. Approach 2 Overview: Hybrid Robot with Arm (HRA)	10
1.2.3. Comparison of the capabilities of the HMR and HRA prototypes	11
1.3. Global System Architecture	11
1.4. Description of the Operation	12
1.4.1. Vision-based Controller	13
2. Hybrid Mobile Robot	13
2.1. Lander/Satellite Hybrid Robot Concept	13
2.2. Aerial Platform (Lander)	14
2.2.1. Avionics Systems	16
2.2.2. First HMR prototypes.	22
2.3. Satellite Design	24
2.3.1. Satellite Architecture	24
2.3.2. Satellite Structure	26
2.3.3. Ultrasonic Sensor	28
2.3.4. Video Feed	29
2.3.5. RC Control	30
2.3.6. Risk Mitigation Testing	31
2.3.7. Energy Consumption	31
2.3.8. Control Range	32
2.3.9. Navigation	33
2.3.10. Thickness Measurement Acquisition	34
3. Hybrid Robot with Arm	35
3.1. Modular Hybrid Robot Concept	35
3.2. Aerial Subsystem Details	36
3.2.1. Airframe Description	38
3.2.2. Avionics systems	38
3.2.3. Payload	39
3.2.4. Motorization and power supply system	40

3.2.5. Fault tolerance functions	40
3.3. Magnetic Bridge Description	41
3.4. Add-Ons Description	46
3.4.1. Clamp Add-on.....	47
3.4.2. Soft Clamp	49
3.4.3. Rollers add-on (racks).....	53
3.4.4. Articulated rover	54
3.5. HRA Stabilisation System using Propellers with Variable Pitch	55
3.6. Robotic-Arm Description.....	58
3.6.1. Fixed Articulation with 180° Probe (FAP180)	58
3.6.2. Anthropomorphic Robotic Arm with 180° Probe (ARAP180).....	59
3.6.3. Anthropomorphic Robotic Arm with 90° Probe (ARAP90).....	61
3.6.4. Snake Arm with pan and tilt Probe (SAP)	61
4. Coverage Analysis with Project Requirements.....	63
5. Conclusions.....	68
References.....	69

List of figures

Figure 1. HYFLIERS architecture.	11
Figure 2. Description of the operation.	12
Figure 3. Left: Encoder/Decoder structure of the neural network. Right: visual estimation of pipe's position and orientation.	13
Figure 4 Block diagram of the HMR	14
Figure 5 Design of the HMR lander and its main elements.....	14
Figure 6 Ramp design	15
Figure 7 Electro-magnet and shock absorber design	15
Figure 8 HMR avionics architecture.....	16
Figure 9 DJI A3 autopilot	17
Figure 10 Jetson TX2 module.....	17
Figure 11 DJI Lightbridge 2.....	18
Figure 12 Depth camera.....	19
Figure 13 Tracking camera	19
Figure 14 LIDAR 3D	20
Figure 15 LIDAR 2D	20
Figure 16 FPV camera	21
Figure 17 Gas sensor.....	21
Figure 18 Prototype of HMR with magnetic landing gear integrated.....	22
Figure 19 Detail of the electromagnets	22
Figure 20 HMR landed over a pipe.....	23
Figure 21 HMR prototype based on LIDAR 2D technology.....	23
Figure 22 HMR based on stereo cameras and lidar 3D.	24
Figure 23: HMR interfaces	25
Figure 24: Satellite system architecture	25
Figure 25: Satellite components overview	26
Figure 26: Adaptation in driving direction	27
Figure 27: Adaptation of magnetic wheels	27
Figure 28: Principle dimensions	28
Figure 29: Roller-probe design	29
Figure 30: Coupling contact force	29
Figure 31: Function model of the satellite	31
Figure 32: Pulling force test.....	32
Figure 33: RC control range test setup.....	32
Figure 34: Navigation path scenarios.....	33
Figure 35: Inspection path scenarios.....	34
Figure 36: B-Scan of an 8-inch tube in longitudinal direction	35
Figure 37: Modular Hybrid Robot Concept.....	36
Figure 38: Layout and dimensions of the proposed solutions.	37
Figure 39: Airframe design	38
Figure 40: Raspberry Pi 2 Model B + Navio2	39
Figure 41: General view of the Magnetic Bridge.	42
Figure 42. Dimensions of the bottom plate of the aerial platform.	43
Figure 43. Dimensions of the top plate of the clamp add-on.	43
Figure 44. Dimensions of the top plate of the rollers add-on.	44

Figure 45. Dimensions of the top plate of the flexible clamp add-on.....	44
Figure 46. Permanent electromagnets.	45
Figure 47. Operation of the permanent electromagnets of the Magnetic Bridge.....	45
Figure 48 State diagram of the electromagnetic attaching system to exchange the add-ons.....	46
Figure 49 Clearance requirements for each add-on	47
Figure 50 Clamp concept	48
Figure 51 Clamp add-on main parts.....	48
Figure 52 Passive elbow mechanism	48
Figure 53. Soft clamp – fixed Version.....	49
Figure 54. Fixed soft clamp design.....	49
Figure 55 final limbs, displacement and stress analysis.	50
Figure 56 Mobile soft clamp system.....	51
Figure 57 Soft mobile landing gear moving over a pipe.....	52
Figure 58 Sequence of autonomous landing using a soft clamp. It can be observed that the gripper has enough strength to pull the UAV towards the pipe to stick to it.	53
Figure 59 Rollers add-on and exploded view.	53
Figure 60 Rollers add-on concept.	54
Figure 61 Articulated rover concept and proof of concept	55
Figure 62(a) Multirotor on a pipe, 2-DoF rotating; (b) propeller with the variable pitch	56
Figure 63. (a) Variable pitch propeller at minimum angle of the blade position; (b) maximum position.	56
Figure 64. Thrust versus rotor angular velocity.....	57
Figure 65 Performance of fixed and variable pitch in stabilisation.....	58
Figure 66 FAP180 design concept	59
Figure 67 FAP 180 use cases	59
Figure 68 ARAP180 design concept and proof of concept	60
Figure 69 ARAP180 use cases.....	60
Figure 70 ARAP90 design	61
Figure 71 SAP design and proof of concept	62
Figure 72 SAP dimensions.....	62

List of tables

Table 1. Video feed system components	30
Table 2. RC control system components	31
Table 3. HRA first approach of mass system distribution.	37
Table 4. HRA aerial motorization and power supply details and performance.	40
Table 5. Magnetic Bridge dimensions.	42
Table 6. Weights of the Magnetic Bridge elements.....	45
Table 7. Add-ons capabilities comparison.	46
Table 8 Limbs optimized angles and lengths.....	50
Table 9 Specifications of two designs of soft clamp system	53
Table 10 Roller add-on mass distribution	54
Table 11: Requirements coverage.....	68

1. Introduction

The objective of the WP2 is to design and develop the prototypes of versatile hybrid robot systems for contact inspection with application to pipe inspection in industrial plants. This document is about the design solution proposed for each platform with their different inspection devices and capabilities.

1.1. Basic Requirements

Apart from the general requirements for an aerial vehicle, which are the capability of taking-off, flying and landing in safety conditions, the user requirements needed to develop the robotic system(s) in the HYFLIERS project are listed in the deliverable D1.1 [1]. In short, these are:

- remote UT inspection of pipes in refineries for loss of wall thickness,
- by a hybrid robotic system able to fly close to the location of interest, land on a pipe and move along the structure to the inspection location and then perform the inspection,
- geometries to be covered (as good as it gets):
 - pipe, elbows, joints,
 - diameter range of DN200 to DN600,
 - single pipe and pipe in pipe racks;
- operation under hot-work permit
 - continuous monitoring of safety of environment (explosive atmosphere),
 - robust emergency behaviour in case of dangerous conditions,
 - able to land safely with one rotor inoperable.

Moreover, the end-users emphasized the importance of developing these robots as small as possible in size and with the capability of interrupting the inspection as fast as possible in case of an emergency in a safe way.

Thus, this document is focused on a design which meets these end-users' requirements taking into account all the constraints and the extra-considerations in terms of size, weight and security.

1.2. Design Approach

To maximise the fulfilment of the industrial requirements and to achieve the set objectives, two unique prototypes following separate approaches will be designed, developed and verified in HYFLIERS.

1.2.1. Approach 1 Overview: Hybrid Mobile Robot (HMR)

This approach is focused on a hybrid robot that can take-off, fly, land and move on a pipe to perform the inspection required by the end-users. This system is focused on the magnetic pipes inspection and it is composed of an aerial vehicle adapted to the industrial environment and a satellite vehicle with the capability of crawling along the pipe to carry out the pipe inspection with the sensors mounted on-board. The details of how this approach works and the design devoted to meet the end-users requirements are presented along Section 2.

1.2.2. Approach 2 Overview: Hybrid Robot with Arm (HRA)

The HRA approach is focused on pipe inspection using a lightweight robotic arm with and UT probe into the end effector and a miniaturised camera to provide close visual images of the surface. The system will be able to land on non-magnetic pipes with different size from 6 inches and could also accomplish the inspection task in pipe racks. These capabilities will be reached through the design of

a modular aerial platform and different add-ons which will be used depending on the application. The details of this approach as well as the different add-ons, the detachable emergency mechanism and the robotic arm are presented in Section 3.

1.2.3. Comparison of the capabilities of the HMR and HRA prototypes

	Approach 1: HMR	Approach 2: HRA
Application	360° inspection of magnetic pipes; possible axial and circular scans	Inspection of any location on the pipe and adjacent location, rather than point measurements
Geometric constraints	The dimensions of the hybrid robot impose constraints on access to the lower part of the pipe racks	Depending on the installed add-on installed, the required clearance between pipes could change. Includes the capability of inspecting pipe racks.
Aerial system	Multirotor	Multirotor, rotors with tilting capabilities to enable lateral propulsion for stabilization on the pipe
Magnetic attractor force	0.3 ... 3x weight	No magnetic force
Axial drive	Motor driven	Motor driven
Circumferential drive	Motor driven	Motor driven or aerial propulsion driven

1.3. Global System Architecture

The architecture scheme of Figure 1 presents a general overview of the complete HYFLIERS system and its components, which is based on deliverable D2.2 [2]. This architecture differentiates the ground system and the aerial system as two main subsystems which are connected through a wireless link while they exchange information about the mission state, the telemetry of the aerial platform and the results of the inspection.

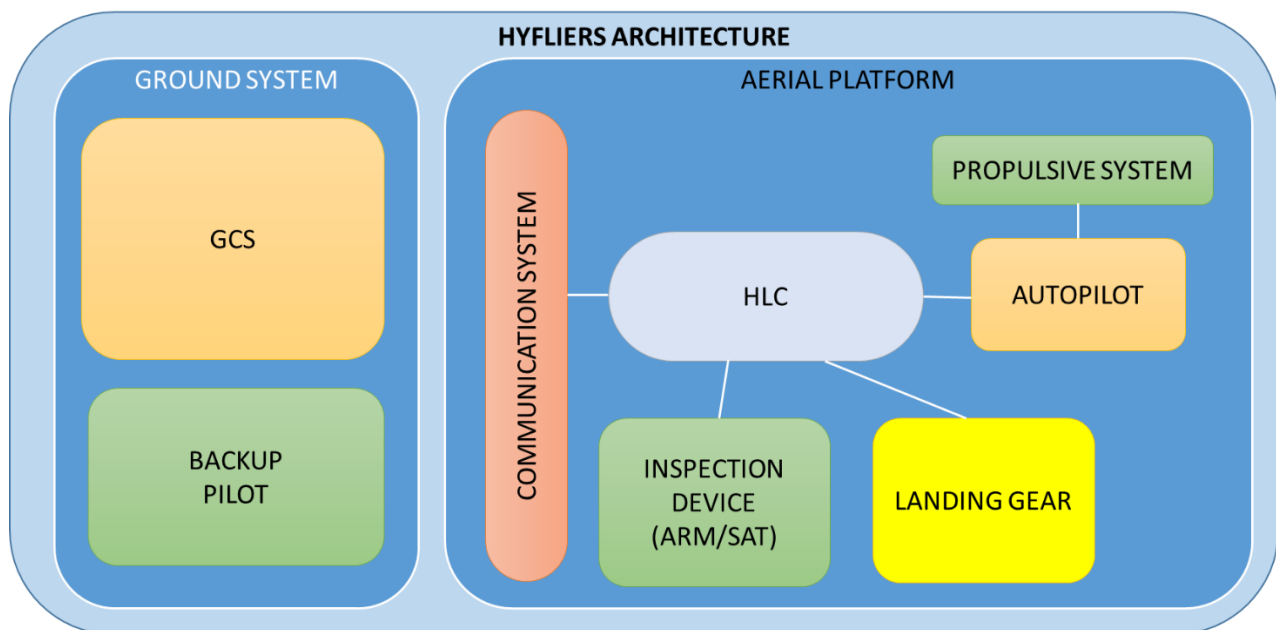


Figure 1. HYFLIERS architecture.

The ground system is composed of a ground control station (GCS), a ground communication system and a remote pilot. The functions of the GCS are ranging from monitoring the mission and the platform state to provide the close visual images collected by the aerial platform to the operators. On the other hand, the remote pilot will have the functions of carrying out the flights in an automatic or semiautomatic mode and will also oversee recovering the aircraft in case of emergency, so the pilot will always be the final decision maker.

The aerial system includes the aerial platform, the autopilot, the communication system on-board and a high-level computer (HLC) which oversees monitoring and controlling the state of the mission and the aerial platform on-board. This computer will also be responsible for collecting the measurements of the inspection tasks as well as running the vision algorithm to detect and land into the pipes. Furthermore, the aerial system will have the inspection device onboard and the actuators needed to guarantee that the aircraft can establish safety conditions landed on the pipe. The autopilot will accomplish the related task related to the estimation of the platform and control of the aerial platform. Lastly, both detachable emergency system and the different add-ons mechanisms are also on-board and controlled by the HLC.

1.4. Description of the Operation

Figure 2 presents a flowchart of the inspection operation for which the HYFLIERS system has been designed. The first part of the operation (from 1-3) could be accomplished in autonomous mode in which the aerial platform approaches the inspection target navigating between different WPs or semi-autonomous mode in which the pilot is the responsible of carrying out this approaching task. Once the platform is hovering close to the inspection target and the pipe is in the field of view of the sensors used for landing, the position control of the aerial platform will be switched to autonomous vision-based control and the autonomous land or perching in the pipe operation is carried out. Then, when the aerial platform has landed, and it is maintaining a stable condition on the pipe the inspection phase starts. In this inspection phase, the small satellite of the HMR or the whole platform of HRA will start to crawl and inspect the pipe. Last, if the inspection is finished, the aerial platform goes back to the safe landing zone or continues to the next inspection target in autonomous or semi-autonomous mode.

In case of emergency, the system will allow switching to a full manually controlled flight by the pilot for landing in a safe area. On the other hand, if the emergency mode is activated during the inspection phase, the aerial platform will detach the inspection device and leave the pipe to minimize the time of taking-off the pipe.

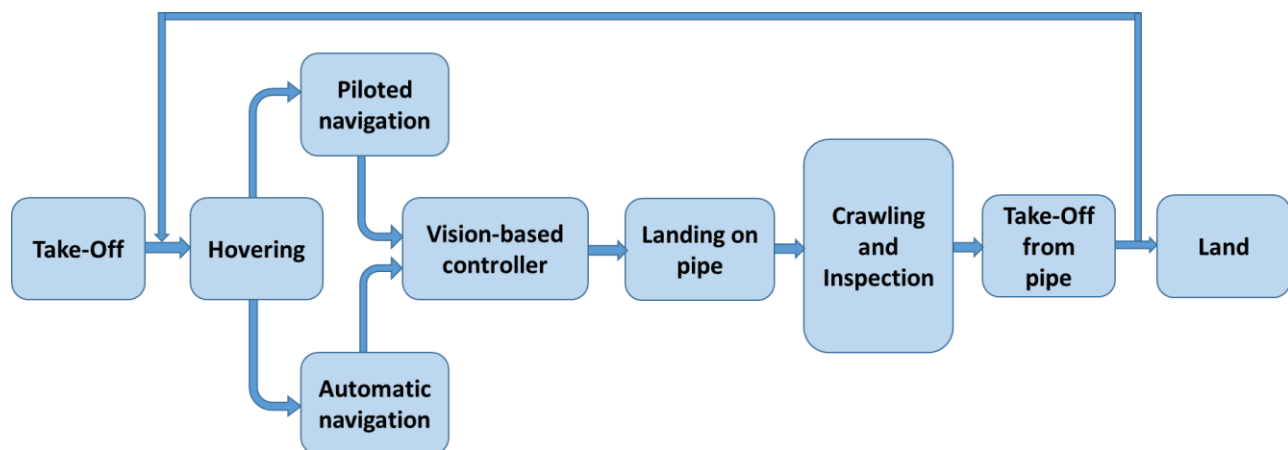


Figure 2. Description of the operation.

1.4.1. Vision-based Controller

This section briefly summarizes the first implementation of the vision-based controller to guide the aerial platforms during the assisted landing operations, which has been presented in [3]. The purpose is to help the pilot to dock the robot to the desired pipe, previously selected by the pilot. The detection algorithm uses the colour and depth images obtained from the Intel RealSense D435 device (see Figure 12). The detection occurs in two stages. At first instance, a convolutional neuronal network (CNN) uses the colour image to perform the segmentation. Then, the segmentation is used with the depth image to estimate the pose of the target pipe accurately.

The CNN used is based on the work presented in [4]. The idea behind it is the fact that grouped convolutions and shuffled channels reduce computational cost while maintaining good accuracy. The result of the network is a mask image, of the same size of the input image, with the segmentation of the different classes. This mask corresponds to the *argmax* function of the probability of the classes. In this case, only two classes are searched, the pipe and the “background”, which will be all the other parts of the image and will be shown as black at the output image.

The *argmax* image given by the CNN is used together with the depth information provided by the depth camera to create a small point cloud with the points that are candidates to belong to the pipe. However, this cloud is susceptible of containing noise points associated with the noise of the depth camera. For this reason, a RANSAC implementation for detecting cylinders is used. This last stage gives a robust estimation of the position and orientation of the pipe which feeds the autopilot.

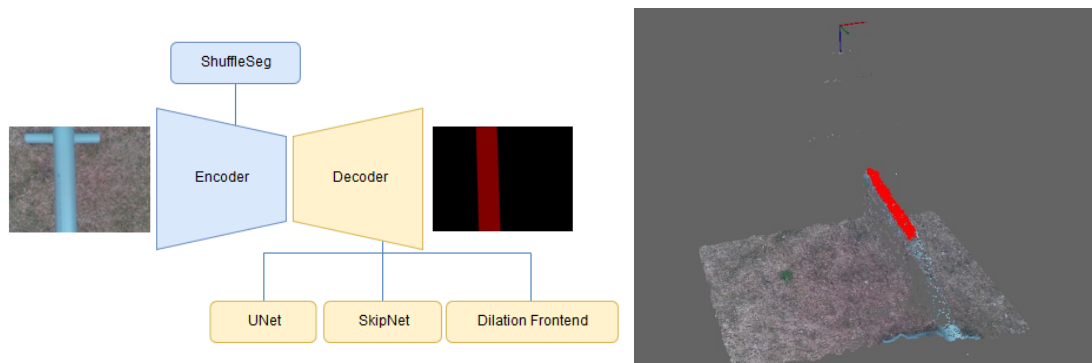


Figure 3. Left: Encoder/Decoder structure of the neural network. Right: visual estimation of pipe's position and orientation.

Figure 3 shows the general structure of the CNN and an example frame with the results of the visual estimation of the pipe's position and orientation. A more detailed description can be found in [4].

2. Hybrid Mobile Robot

The HMR approach consists of a hybrid robot which can flight and crawl over the pipe while the inspection of magnetic pipes is being accomplished. This will be reached using an integrated system composed of an aerial platform and a self-propelled semi-independent satellite which has an UT roller probe to accomplish the inspection application.

2.1. Lander/Satellite Hybrid Robot Concept

The main novelty of the design concept of the HMR is that it is composed of two semi-independent subsystems: the aerial platform and the self-propelled satellite. Both subsystems have been designed with different but complementary functionalities to meet the requirements of the end-users.

First, the lander is the aerial platform which is in charge of placing the satellite on a target pipe selected by the inspection operator. This system has not been designed with inspection capabilities; however, its function is essential to transport and deploy the inspector satellite over the pipe. Then, the satellite must be able to navigate along pipes and elbows of diameters ranging from 200 to 500 mm (8 to 20 inch) using magnetic wheels to maintain the attraction force between the magnetic pipe and the twin-crystal roller-probe used to carry out the inspection task.

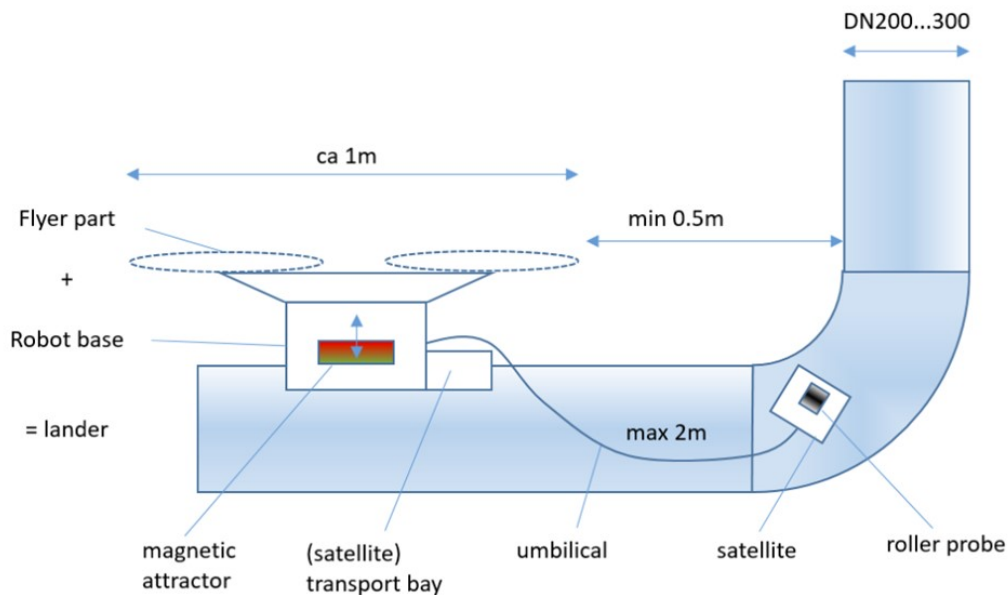


Figure 4 Block diagram of the HMR

2.2. Aerial Platform (Lander)

Figure 5 shows the current design of the aerial platform of the HMR (lander), which is composed of a Flyer and a Robot base and its main parts.

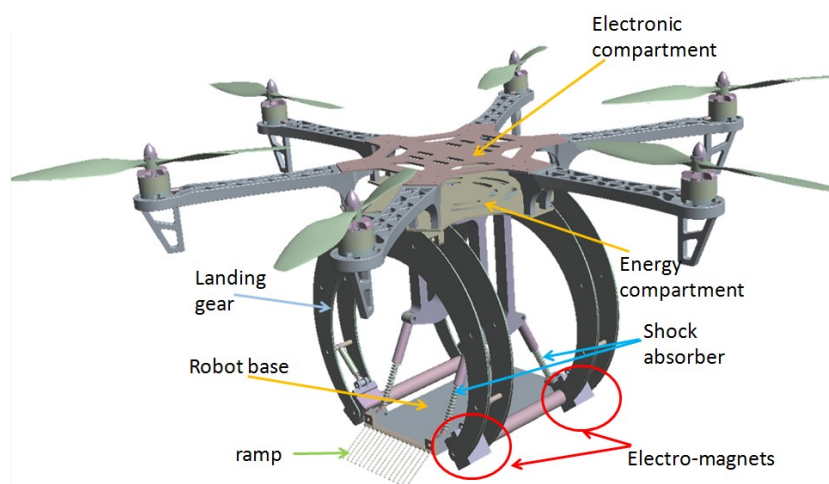


Figure 5 Design of the HMR lander and its main elements

As it can be seen in Figure 5, the main components of the current HMR design are the following:

- Electronic compartment: Over the top of the platform are integrated the autopilot, the PC and the main sensors. It is important to note that the cameras and LIDARs must be placed with a specific orientation that depends on their functionalities so that several adapters will be added to this top.
- Energy compartment: Batteries and the energy management system are installed in this compartment.
- Landing gear: The landing gear has been designed considering the size and weight of the satellite robot. Currently, it consists of four legs. However, it is being studied the possibility of replacing this design by a three legs prototype.
- Robot base: It consists of a magnetic ramp that transports the satellite robot.
- Ramp: It is a magnetic ramp, deployed during the inspection operation to facilitate the attachment of the satellite robot to the pipe. Figure 6 shows the design of this part of the HMR.

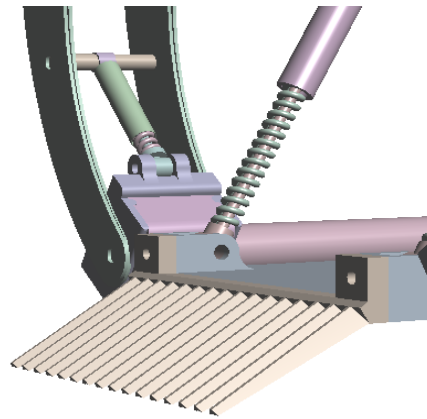


Figure 6 Ramp design

- Electro-magnets: The electromagnets are employed to attach the HMR to the pipe during the landing maneuver. In this design, the electromagnets can rotate to adapt their orientation according to the pipe's shape. Figure 7 presents an electromagnet attached to the landing gear.

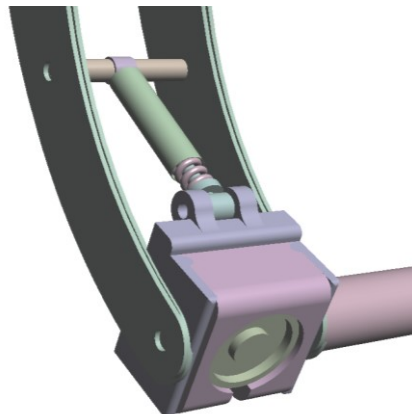


Figure 7 Electro-magnet and shock absorber design

- Shock absorbers: The shock absorbers are installed to limit the impact on the robot base when the HMR lands and touches the pipe.

2.2.1. Avionics Systems

The avionics mounted in the lander of the HMR is composed mainly by the autopilot, the propulsion system, the landing gear, the sensors and the energy management system. Figure 8 shows a more detailed scheme of the devices onboard of the HMR lander.

In the first stage of the project, it is planned to test several combinations of all the sensors presented in Figure 8. Based on the obtained results, these sensors can be removed or replaced.

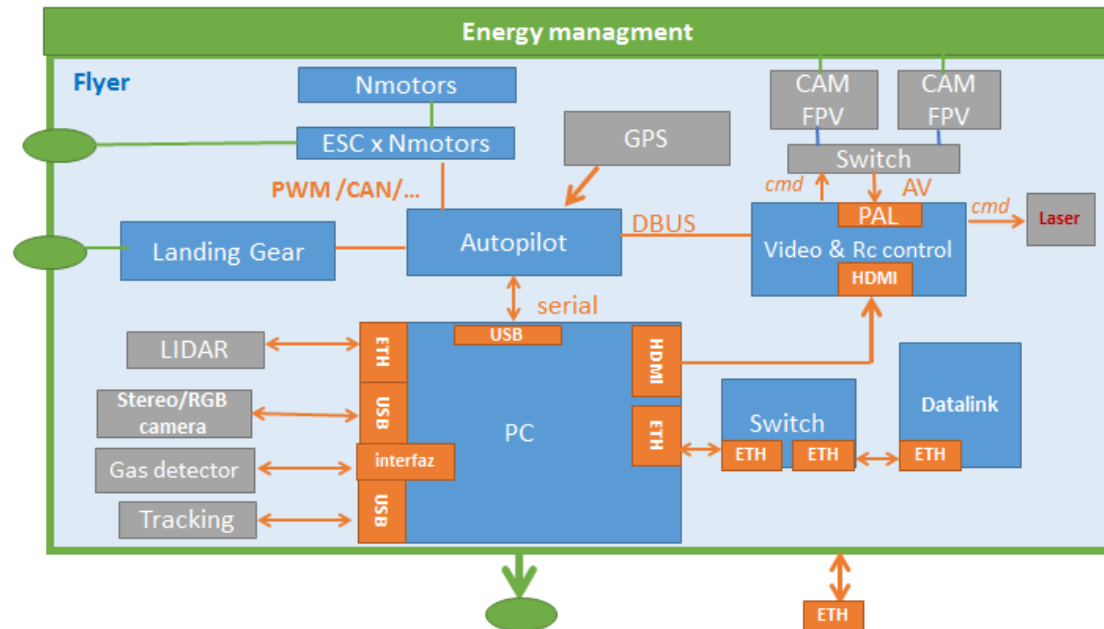


Figure 8 HMR avionics architecture

A description of the selected systems for this architecture is presented in the following subsections.

Autopilot and HCL

As it was presented in the global system architecture in Section 1.3, for controlling and guiding the HMR, there will be two different modules: the autopilot and the HCL.

The chosen autopilot for this robot has been the DJI A3. This system is optimized for professional applications, so it will assure that the TRL remains high. The A3 flight controller is characterized by a strong control determination. Its multi-sensor fusion algorithms improve its control's accuracy by far when compared to other autopilots. The device also includes a robust control algorithm which enables the A3 to be adapted to a wide range of aircraft without the need for manual tuning. One of the most interesting characteristics that this autopilot provides to the HMR is the fault-tolerant control system embedded in this system, which allows landing safely to a hexacopter or octocopter, even in the event of propulsion system failure.



Figure 9 DJI A3 autopilot

The HLC will be used mostly during the landing phase. In this case, the computer receives the camera and LIDAR measurements, processes this information and sends the control commands to the autopilot; it also can receive commands from the operator at the GS through the Datalink. This computer is one of the fastest, most power-efficient embedded computing device in the market. It's built around an NVIDIA Pascal™-family GPU and loaded with 8GB of memory and 59.7GB/s of memory bandwidth. It features a variety of standard hardware interfaces that make it easy to integrate any functions and sensors as needed for the project. Its main specifications are the following:

- GPU: 256-core NVIDIA Pascal™ GPU
- CPU: Dual-Core NVIDIA Denver 2 64-Bit CPU + Quad-Core ARM® Cortex®-A57 MPCore
- Memory: 8GB 128-bit LPDDR4 Memory
- Storage: 32GB eMMC 5.1
- Power: 7.5W / 15W

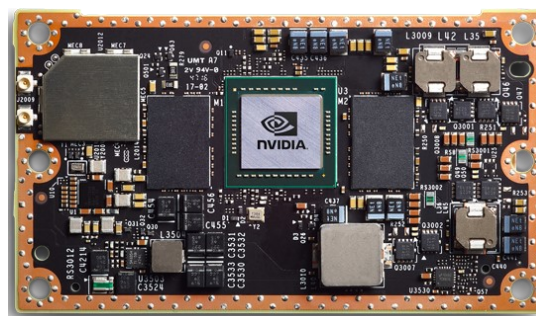


Figure 10 Jetson TX2 module

Radio-Link and communications system

For the radio-link and communication system it has been chosen a DJI Lightbridge 2 module. The Lightbridge 2 has two main roles: In one hand, it provides the communication link between the GCS, RC transmitter and the autopilot. In the other hand, it is a wireless HD video transmitter that enables video streaming to a wide variety of devices, at the same time that it is able to transmit the analogue

video from an FPV camera. In this way, the aerial images and commands can be transmitted with very low latency at a high range. Between its key features are:

- Integrated remote controller
- Low latency as low as 50 ms
- video transmission range of up to 5 km
- Comes with SDI port and mini-HDMI port
- Can stream video from two cameras simultaneously
- Responsive navigation and intelligent algorithms
- Multiple remote controllers
- 6000mAh of battery for longer operational time
- Master-Slave mode
- The controller comes with the USB, 3G-SDI ports and mini-HDMI that support the broadcast output of 720p/59.94 fps and 1080i/50 fps, the video output of up to 1080p/60 fps.



Figure 11 DJI Lightbridge 2

Motorization and Power Supply

Lithium-Polymer (LiPo) batteries have been chosen for the power supply of the HRM. The main reasons for this choice are their low weight, high energy density, and low discharge rates. In this way, the power supply of this system will consist of a set of 6S LiPo batteries. This means that the battery will have six cells where each cell has a nominal voltage of 3.7 volts (4.2 V fully charged). The total pack voltage is $6 \text{ cells} \times 3.7 \text{ V} = 22.2 \text{ V}$.

Regarding the motors, they will be chosen with the following assumptions:

- Maximum take-off weight = 12 kg
- Satellite robot + components = 2 kg
- Other elements (weight margin) = 500 g
- Motor efficiency = 9
- Power in the working point = 166.

Sensors

Following, several sensors which had been tested are presented:

- **Depth Camera**

The depth camera is being tested for obstacle avoidance and for the landing phase. Due to this device is able to providing images, depth maps and point clouds, it is a good option for use in the computer algorithms during a pipe landing operation. The selected camera is the Intel Real Sense 435 I (low-weight camera of 72 g).



Figure 12 Depth camera

- **Tracking camera:**

This camera is necessary for performing the localization task in scenarios where the GNSS is not available. For the HMR, it has been chosen a light-weight tracking camera (55 g) that performs a SLAM algorithm internally. The integrated model is the Intel RealSense Tracking Camera T265. It includes two fisheye lens sensors, an IMU and an Intel Movidius Myriad 2 VPU. All of the V-SLAM algorithms run directly on the camera, allowing for very low latency and extremely efficient power consumption. It offers sub 6ms latency between movement and reflection of movement in the pose.



Figure 13 Tracking camera

- **LIDAR:**

Lidar technology will be used for obstacle avoidance and landing control. These sensors provide very accurately (up to 2 cm) point cloud measurements at very high rates. Now, two different LIDARs are being tested, depending on the results obtained during the test phase, one of them will be chosen and integrated into the Flyer. The first one is the 3D multibeam LIDAR Ouster OS-1 of 16 channels. It weighs 396 g, has a range of 120m and can measure up to 327.680 points per second.



Figure 14 LIDAR 3D

The second LIDAR is the Hokuyo UST-10LX. This is a small and low weight (130 gr), accurate, high-speed device. This model uses Ethernet interface for communication and can obtain measurement data in a wide field of view up to 10 meters with millimeter resolution. Due to its low power consumption, this scanner can be used on battery-operated platforms. This sensor uses a laser source to scan a 270° field of view. Positions of objects in the range are calculated with step angle and distance.



Figure 15 LIDAR 2D

- **FPV Cameras**

These cameras will be used for First Person View control of the flyer. They have been chosen as analogue because this kind of video does not have too much delay, so it is possible a good remote control. The model chosen for the integration is the Foxer Falkor Mini. It's designed as an all-around camera that would work well under different lighting conditions. The Foxer Falkor is switchable in the menu between 16:9 and 4:3 aspect ratio and PAL/NTSC video formats in the settings, which makes it a great option for all FPV goggles and displays. Its main properties are the following:

- 1200TVL CMOS Image Sensor
- Supports OSD: Pilot name, battery voltage, timer
- Min. Illumination: 0.01Lux
- Supports Color and B&W
- Input Voltage: 5V – 40V
- Dimension: 28x26mm
- Weight: 13.5g



Figure 16 FPV camera

- **Gas Sensor:**

Gas sensor will be used for detecting emergency situations. Currently the main option for this system is the GasCard NG sensor, however this decision may not be definitive. The GasCard NG infrared gas sensor is designed for ease of integration with a wide range of gas detection systems that require high quality, accurate and reliable measurement of CO, CO₂, CH₄ gas concentrations. It is set up for single use gas measurement at a time.

It includes real-time temperature and atmospheric pressure correction via onboard sensors and has the flexibility to incorporate additional gas detection technologies. It has onboard true RS232 communications along with the option of TCP/IP communications protocol. Its weight is approximately 300 g.



Figure 17 Gas sensor

2.2.2. First HMR prototypes.

In this section are presented the first prototypes integrated for testing the different technologies that are being developed for the HMR Lander. Figure 18 and Figure 19 show the real implementation of the design presented in the previous section using a DJI F550 aerial frame.

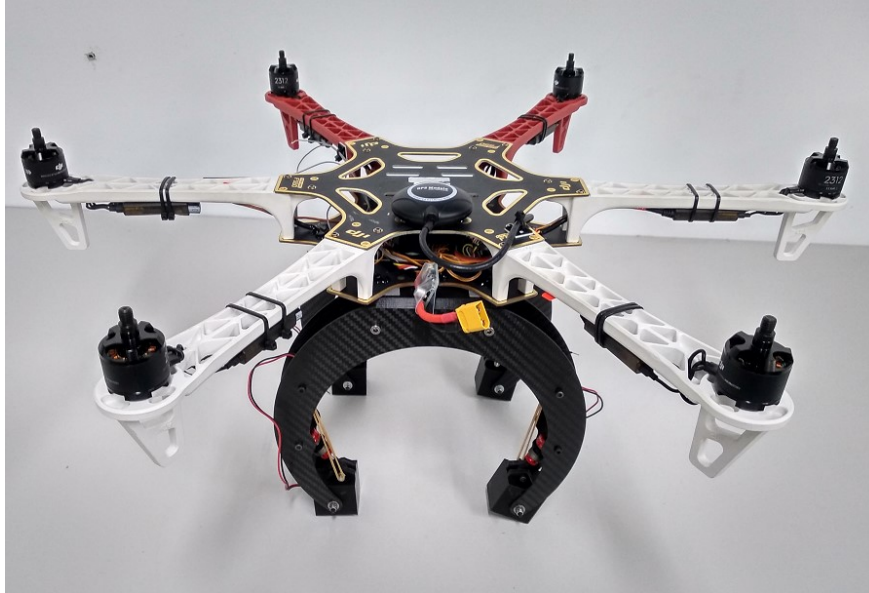


Figure 18 Prototype of HMR with magnetic landing gear integrated



Figure 19 Detail of the electromagnets

In some of the tests performed until now, it has been possible to land correctly (see Figure 20). However, it has been detected that the landing manoeuvre could be carried out more accurately by replacing the four-point landing gear with a three-point one. This decision will be considered as we perform more tests.



Figure 20 HMR landed over a pipe.

Regarding the sensors, we are currently working in two different approaches for accomplishing with the object avoidance block and the landing phase:

- a) The first prototype is based on lidar technology. Based on the scans of the lidar, it is possible to avoid the obstacles around the HMR during the navigation. For the landing phase, the lidar is placed looking down. Because this LIDAR is 2D, the scans show a section of the pipe and it is possible to centre the robot over the pipe. In this case, the computational consumption is low, so by using this configuration, it should be possible to use low grade and low-weight computers for this operation. Figure 21 presents the prototype with a 2D LIDAR integrated and oriented for the landing phase.

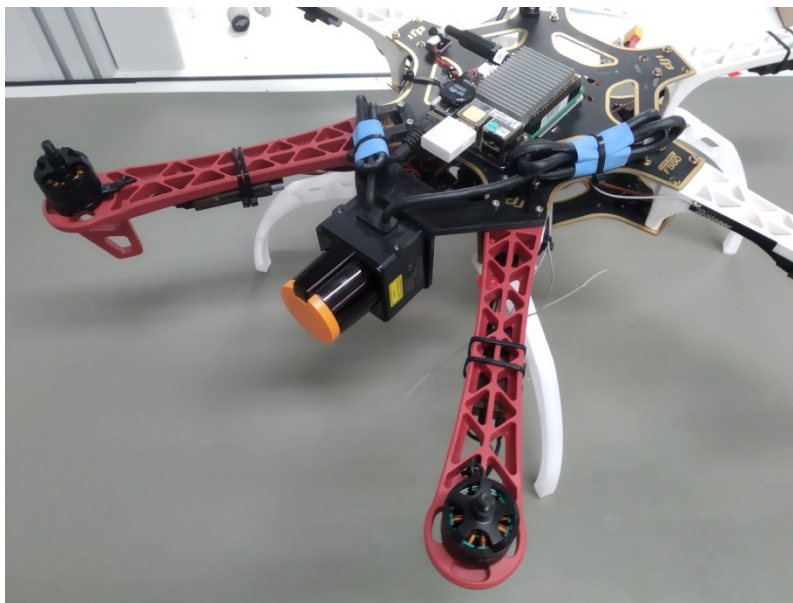


Figure 21 HMR prototype based on LIDAR 2D technology

- b) The second prototype is based on 3D LIDAR and depth cameras technology. The 3D LIDAR is placed on top of the HMR and can see everything around the multirotor, which is very useful for detecting the possible obstacles. Currently, two different depth cameras have been

installed on this model: the first one is facing up and is used for avoiding obstacles when the robot take-off; the second one is facing down and it is used for obtaining cloud points which allow creating a model of the pipes and control the landing phase of the platform. This model of the pipes can also be obtained with the lower layers of the 3D Lidar scan.



Figure 22 HMR based on stereo cameras and lidar 3D.

2.3. Satellite Design

To meet the user requirements within the HMR system concept, the satellite has to be able to navigate tubes and elbows of diameters ranging from 200 to 500 mm (8 to 20 inches). Both circumferential and longitudinal movement along pipes is required to reach any desired inspection location. The tether (umbilical) to the satellite must allow enough range to access locations closer to larger structures while allowing the HMR lander to keep a safe distance from anything that might interfere with flight or landing operations. The movement of the satellite shall be controllable from up to 100 meters distance. The total weight of the robot shall stay under 1.5 kg, ideally below 1.0 kg, to allow the HMR to meet flight time and mission duration requirements. The satellites primary function is to carry an ultrasonic probe for wall thickness measurements. The sensor is an ultrasonic dry-coupling 5 MHz twin-crystal roller-probe. The UT-unit is located on the lander. Transmitter and receiver analogue signals must be routed between instrument and probe over a 2 m umbilical between lander and satellite. To compensate for cable length, a preamplifier is to be placed on the satellite to boost the return signal. Inspection locations might be on straight pipe and elbow section. The satellite must be able to acquire continuous line scans and provide accurate relative position information.

2.3.1. Satellite Architecture

Figure 23 describes the interfaces between lander, satellite and remote. The satellite robot carrying the ultrasonic thickness measurement sensor is tethered to the HMR Lander for power supply, ultrasonic analogue signal transfer and incremental position information. The ground-side remote for steering and video feedback is connected through two radio links between the satellite and the handheld RC controller with an attached video display.

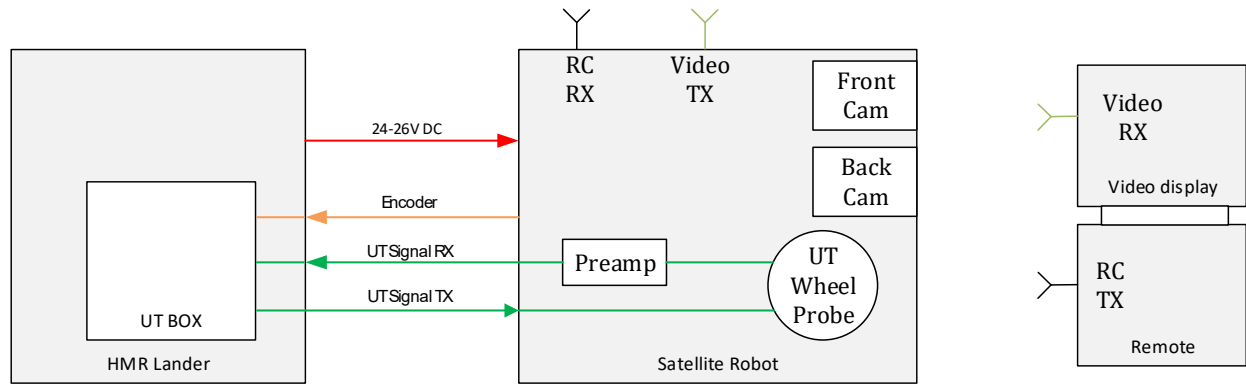


Figure 23: HMR interfaces

The detailed block diagram of the satellite robot is shown in Figure 24. It is equipped with two brushless DC motors, which are controlled by GEIR motor drivers. Incoming RC speed control signals are directly routed from the RC receiver to the motor controllers. An analogue switch controlled over the RC remote connection allows toggling between two cameras. The UT signal transmitter cable from the lander is directly routed to the roller probe, while the receiver connection first goes through a preamplifier to improve signal quality before being passed on back to the lander and its UT instrument. An incremental encoder is connected to one of the motor drivers for power supply. The encoder A and B signals are routed on through the umbilical to the UT instrument on the flyer.

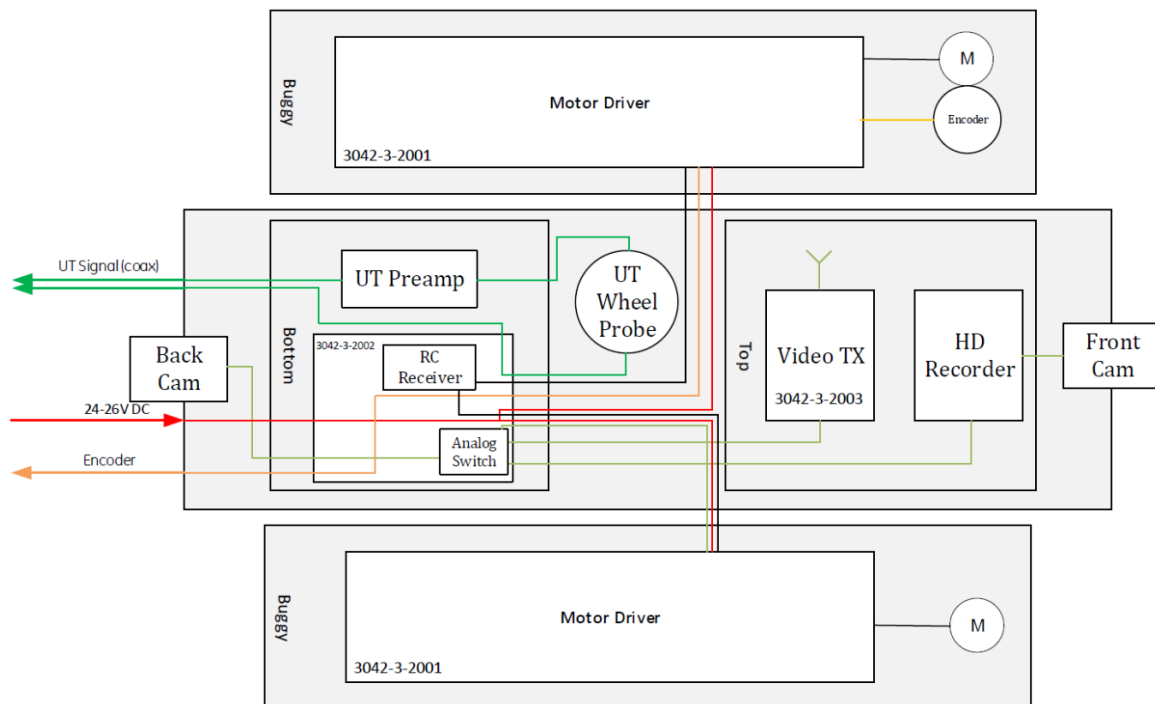


Figure 24: Satellite system architecture

2.3.2. Satellite Structure

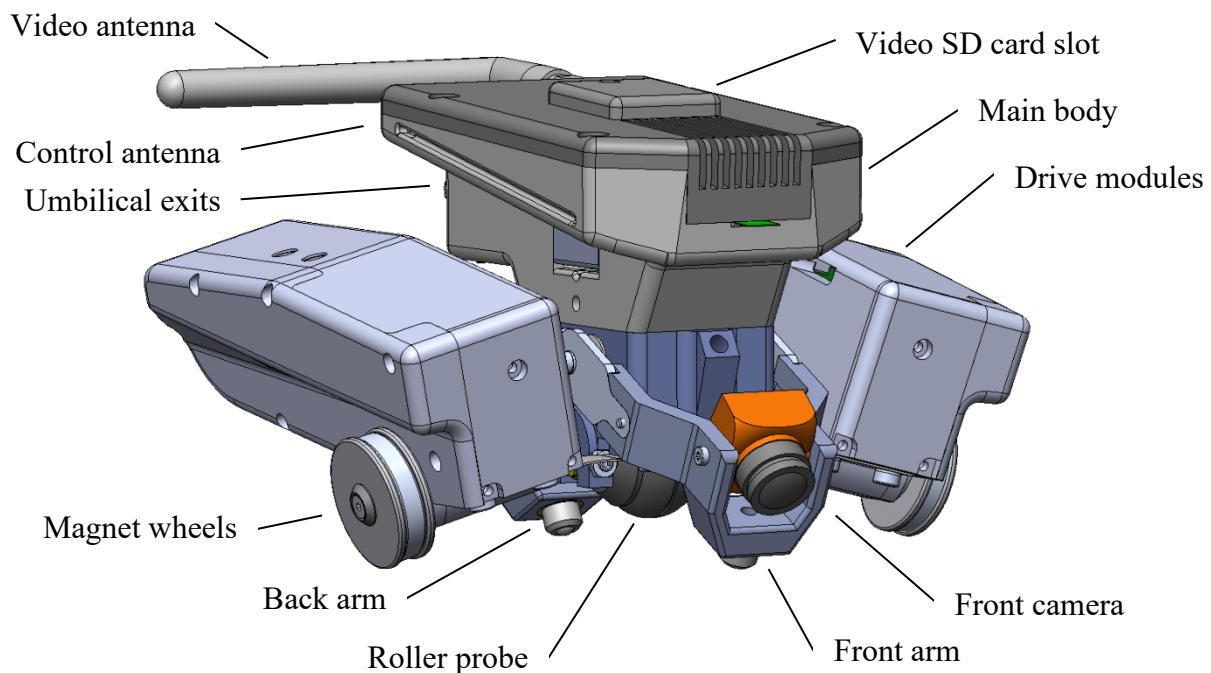


Figure 25: Satellite components overview

Figure 25 gives an overview of the main system components of the satellite.

Each drive module houses a brushless DC motor with a planetary gearbox. A worm gear transmission connects the motor axis to the wheel axis. A GEIR motor driver in each module allows short cables to the motor windings to avoid potential electromagnetic interference with the inspection equipment. An additional incremental rotary encoder is placed on the motor axis and directly wired through the umbilical to UT acquisition instrument on the flyer.

The magnet wheels are large neodymium ring magnets with steel discs on each side to form a rotationally symmetric horseshoe magnet. They are mounted in a cantilever position to enable easy exchange of application-specific wheels.

The lower main body houses the roller-probe ultrasonic thickness measurement sensor. An absorbent sponge in a pocket over the probe stores and continuously applies a coupling film. The sponge is appropriately sized to provide enough coupling for at least one mission. An accessible coupling connection allows resupply before each flight.

The upper main body is an electronics box for the communication equipment and preamplifier. Accordingly, the RC receiver antenna and the video transmitter antenna are mounted on this box. All interface cables to the lander exit the satellite through this box.

The front and back stabilizer arms are mounted on the main body. They are equipped with ball rollers for both forwards and sideways movement. Their rollers are backed by strong permanent magnets to counteract the motor momentum. Additional leg springs may be added between the arms and the main body. The forwards and backwards cameras are mounted on the arms to adapt their field of view based on the curvature of the surface.

In the driving direction, the satellite can adapt and clear outer diameters of 200 mm (8 inches) and inner diameters as small as 300 mm as shown in Figure 26. Figure 27 shows the range of motion of the magnetic wheels. It can adapt to convex diameters of 200 mm and concave diameters of 300 mm.

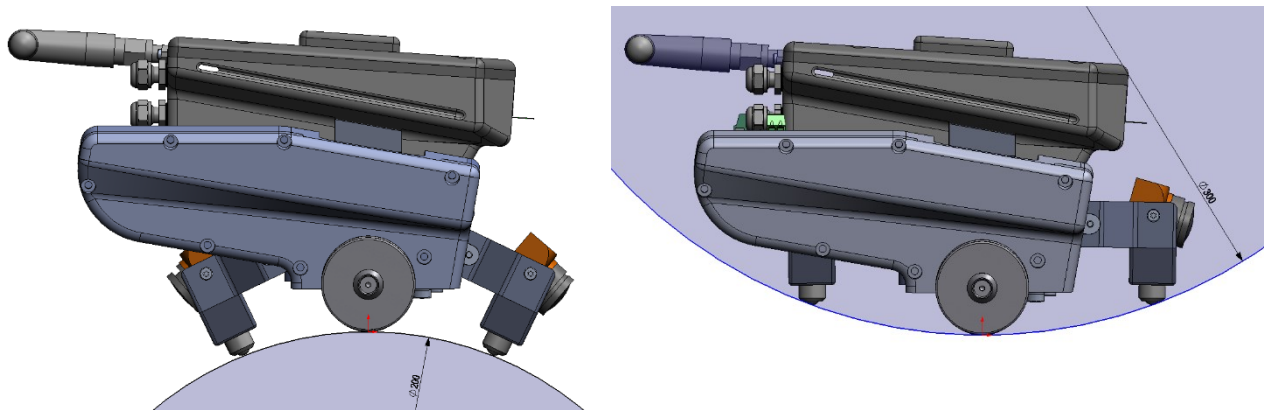


Figure 26: Adaptation in driving direction

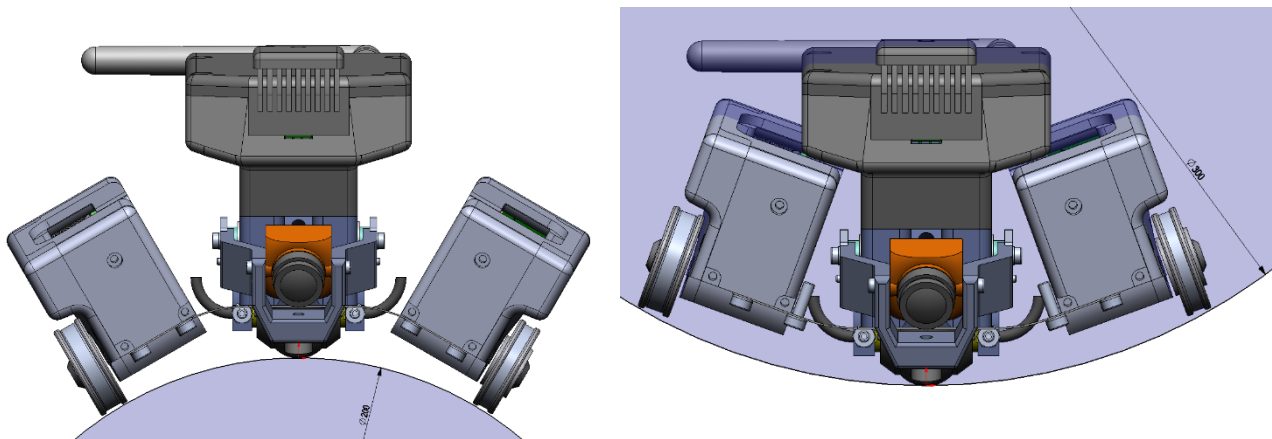


Figure 27: Adaptation of magnetic wheels

Any combination of these two degrees of freedom is possible when navigating geometries more complex than movement along or around a single tube.

The satellite height allows it to move through clearances between pipes as low as 100 mm.

System specifications

Satellite		
Speed	mm/s	100
Weight	kg	0.8
Power supply	V	24 ... 26
Peak load	W	28.5
Size W x L x H (Figure 28)	mm	138 x 171 x 90
Min. height clearance	mm	100
RC control range	m	100
Umbilical length	m	2
Video feed		HD 1080p
Protection rating		IP 3x

Test specimen		
Diameter range for navigation	mm	OD 200 ... ID 300
Diameter range for inspection	mm	OD 200 ... flat
Surface temperature	°C	0 ... 80
Max. coating thickness	mm	0.3
Material types		C-Steel
UT Transducer		
Material thickness range	mm	5 ... 100
Transducer frequency	MHz	5
Coax plug		Lemo 00
Encoder type		Incremental quadrature
Encoder resolution	cnts/mm	424
Encoder plug		Lemo 0B.306

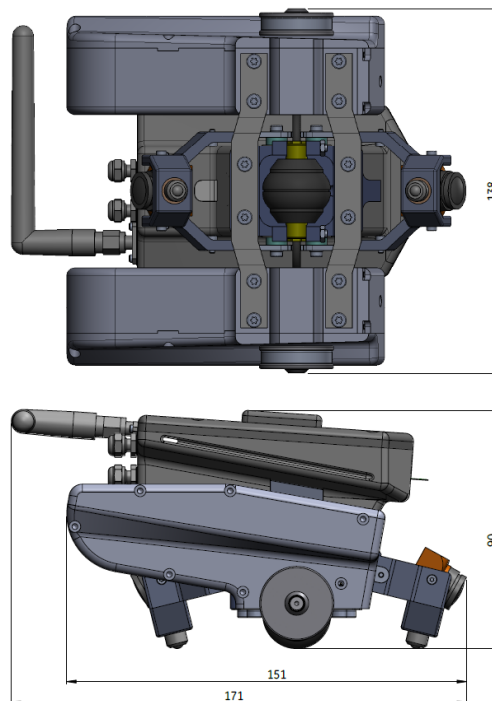


Figure 28: Principle dimensions

2.3.3. Ultrasonic Sensor

A twin crystal pulse-echo probe is placed on the satellite (Figure 29). It is embedded in an axis facing laterally outwards. A freely turning elastomer tire is suspended on the axis to transmit the ultrasonic wave from the probe face to the inspection sample. Although this design is classified as dry coupling, a light oil film should be applied to the surface of the rubber tires.

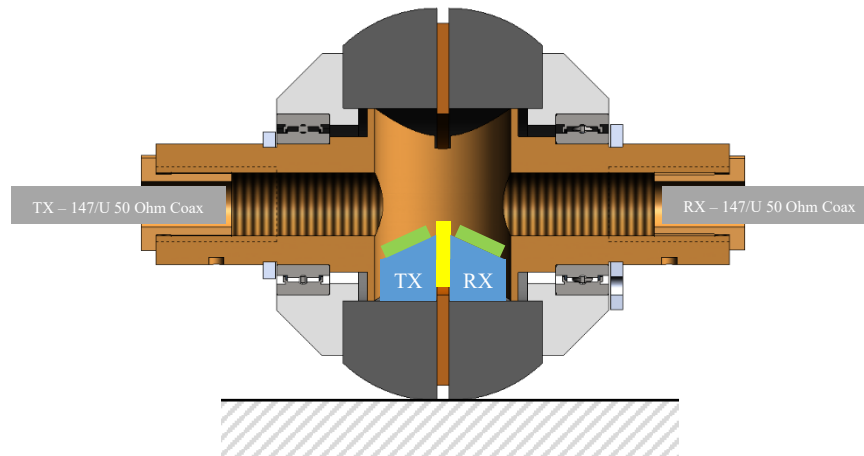


Figure 29: Roller-probe design

Sufficiently high contact forces are necessary to deform the rubber tire to generate a circular contact area to the inspection sample. Any remaining air gap due to surface roughness must be filled by coupling fluid. Figure 30 depicts how the robot generates this force through deformation of the flat spring suspension of the two magnetic wheels. The resulting counterforce on the central contact point is used for coupling.

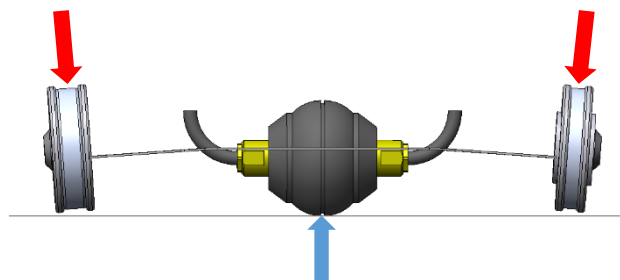






Figure 30: Coupling contact force

A minimal contact force must be achieved when driving on flat surfaces. Smaller outer diameters will increase the contact force due to higher deflection of the flat springs. The soft rubber tire will deform based on the applied force resulting in varying distances between the probe face and inspection sample. Thickness measurements between the excitation pulse and first backwall echo (Mode 1) are therefore not feasible. Instead, it is necessary to measure the distance between two backwall echoes (Mode 3) to compensate for the unknown state of the tire.

2.3.4. Video Feed

Table 1 lists the individual components chosen for the video feed system as laid out in the system architecture described in Figure 23.

Table 1. Video feed system components

Camera	Video Transmitter 5.8 GHz	Video Antenna	Video Receiver 5.8 GHz
			
RunCam Split Mini 2	Team Black Sheep Videosender Unify Pro 5G8 RPSMA V2	ImmersionRC SpiroNET V2 5.8GHz RHCP	Graupner FPV DVR Monitor 7" 5,8 GHz Diversity
<ul style="list-style-type: none"> • Size: 19 x 19 mm • 1080P/60fps HD recording & WDR FPV camera • Weight: 12.5g • Voltage Range: 5 - 20V • FPV aspect ratio 16:9/4:3 switchable 	<ul style="list-style-type: none"> • Operating Voltage: 4.5-5.5V • Dimensions: 18(H) x 25(W) x 4(D) mm • Supply current: up to 600mA • Weight: 5g • Up to 800mW of output power 	<ul style="list-style-type: none"> • 5.8GHz Band • Circular Polarization • Fully protected against the elements • Individually tested • Connector: SMA • Size: 33.5 x 16 mm • Weight: 11.5g 	<ul style="list-style-type: none"> • Screen: 7" TFT LCD monitor, LED backlight, 800 x 480 pixels • Size: 184 x 126 x 28 mm • 1800mAh LiIo battery • Weight: 500g

2.3.5. RC Control

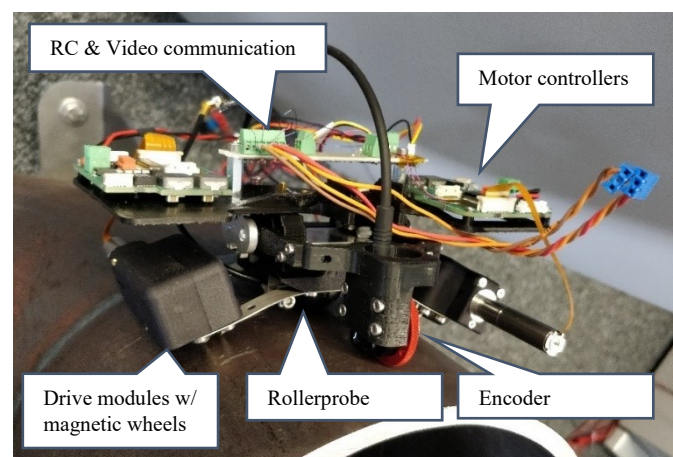
The operator uses a RC remote to control the robot. A program running on the remote translates the user's input into appropriate speed values for each of the two satellite drives. These signals are wirelessly sent to the RC receiver on the robot. It directly provides the speed value to each of the motor controllers in the form of a PPM signal. The PPM signal is converted to analogue voltage and fed back into the motor controller which is used as a speed set-point scaler. Table 2 shows the specific components chosen for the task.

Table 2. RC control system components

RC Transmitter 2.4 GHz	RC Receiver 2.4 GHz
	
FrSky Horus X10	
<ul style="list-style-type: none"> • Weight: 980g • LCD: 480x272 • Li-ion battery • 16 channels 	<ul style="list-style-type: none"> • 21.1 x 17 x 7.3 mm • Weight: 2.9g • Voltage Range: 3.5 - 10V • Current: 100mA@5V • 16 channel (1-6 CH PWM)

2.3.6. Risk Mitigation Testing

The functional model (FuMo) in Figure 31 has been built to mitigate requirements risks. It included the full kinematic model with motor driven magnetic wheels. The motor drives, cameras, RC remote-control and video transmission equipment was mounted on-board. The roller-probe could be installed to evaluate the coupling and stability by assessing the signal quality. An absorbent cotton piece allows the continuous application of an oil film on the roller-probe. An encoder is attached to one arm to enable recording of B-Scans.

**Figure 31:** Function model of the satellite

2.3.7. Energy Consumption

To measure the energy consumption, the test setup as depicted in Figure 32 has been built. It consists of a vertical tube section of 1.0037 carbon steel with a diameter of 200 mm. A spring scale attached

to the bottom of the satellite measures the pulling force F_{Pull} . The corresponding current drain was monitored on a laboratory power supply.

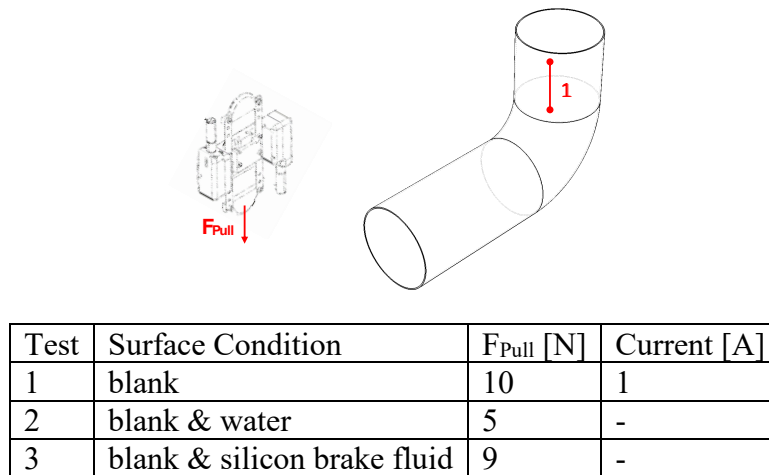


Figure 32: Pulling force test

The maximum measured current under these test conditions was 1 Ampere at 24 Volt supply, resulting in an energy consumption of 24 Watts. Missing from the test setup was the UT preamplifier with 2.5 Watts and the second camera with 2 Watts, resulting in a peak power draw of 28.5 Watts. During flight, the motors may be deactivated to reduce the standby energy consumption to a maximum of 12 Watts.

2.3.8. Control Range

The RC communication has been successfully tested up to a range of 175 meters. Figure 33 shows the respective location of the RC transmitter and receiver.

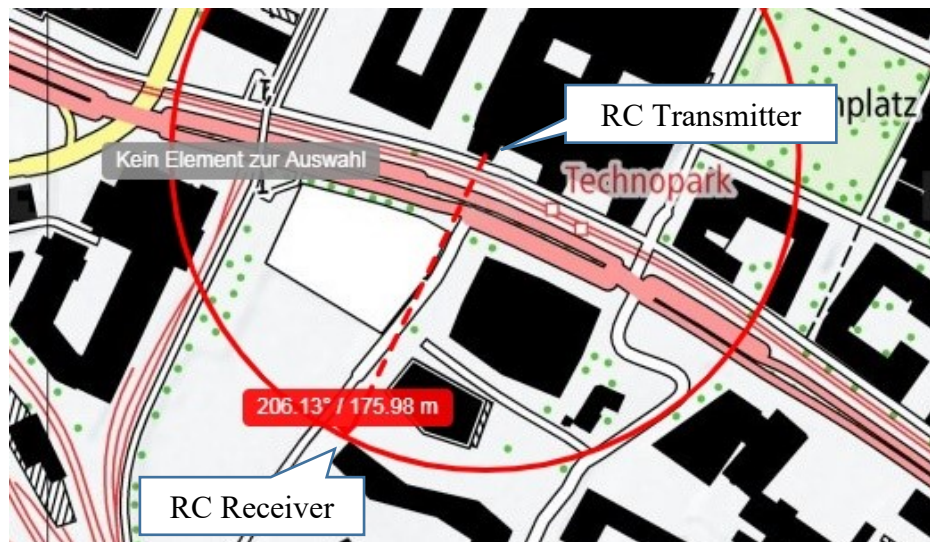


Figure 33: RC control range test setup

These results meet the requirement of a 100 meters remote control range.

2.3.9. Navigation

To test the navigation capabilities of the functional model, several movement paths were determined (Figure 34) to check any situation the robot may encounter in the field. All tests were carried out on a blank dry surface of a 200 mm (8 in) diameter pipe with a wall thickness of 6.3 mm. The elbow radius is equal to 1.5 times the pipe diameter.

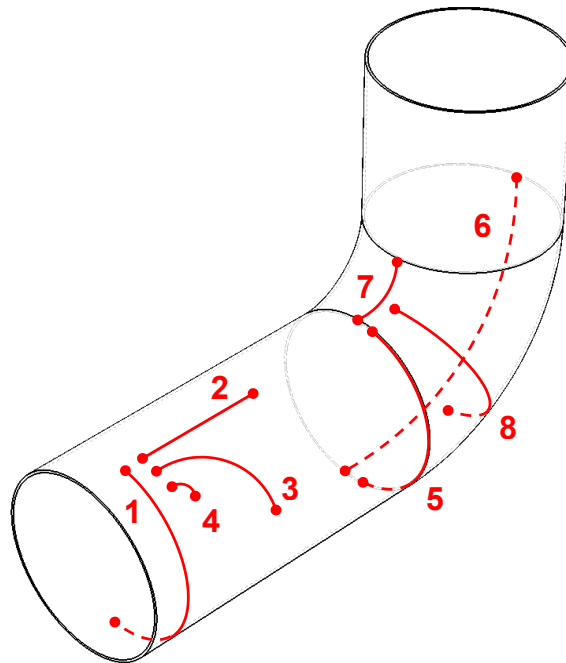


Figure 34: Navigation path scenarios

A result is considered passed if the satellite can be manually steered along the predetermined path to an accuracy of ± 10 mm. Close-up line of sight to the robot is permissible.

No.	Description	Result
1	Moving on a tube between 12 o'clock to the 6 o'clock position in circumferential direction	Pass
2	Moving along the tube in longitudinal direction	Pass
3	90° turn in an arc from longitudinal to circumferential direction with a turning radius of 1,5 times wheel spacing	Pass
4	90° spot turn from longitudinal to circumferential direction	Pass
5	Moving along the circumferential seam between tube and elbow from 12 o'clock to 6 o'clock	Pass
6	Moving in longitudinal direction along the outermost point of the elbow	Pass
7	Moving in longitudinal direction along the innermost point of the elbow	Kinematics can adapt, but motors cause a collision.
8	At 45° along the elbow, move in circular direction from 12 to 6 o'clock	Pass Probe partially loses contact.

For the next satellite iteration, the drives will have to be angled upwards to enable navigation of path 7. No additional actions will be taken regarding the result of test 8, as navigation is possible and line scans could be done on path 7.

2.3.10. Thickness Measurement Acquisition

Several line scan paths (Figure 35) were determined based on the project requirements and additional expected failure mechanism on process piping. All tests were carried out on a blank dry surface of a 200 mm (8 in) diameter pipe with a wall thickness of 6.3 mm. The elbow radius is equal to 1.5 times the pipe diameter.

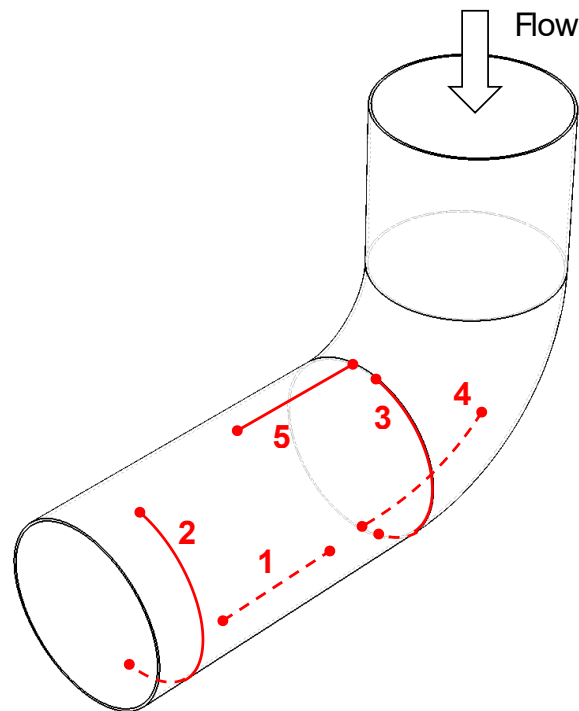


Figure 35: Inspection path scenarios

A result has been considered passed if the ultrasonic A-Scan signal is showing two clearly identifiable back-wall echoes over the entire length of the line-scan.

No.	Description	Result
1	In long. direction at the 6 o'clock position for 150 mm	Pass
2	Circumferentially from 12 to 6 o'clock	Pass
3	On the circumferential seam between tube and elbow from 12 to 6 o'clock	Pass
4	In long. direction along the outermost point of the elbow	Pass
5	In longitudinal direction aligned to the innermost point of the elbow for 45°	Pass

Significant variations in time of flight to the first back-wall echo have been observed between and within individual line-scans. Signal amplitude is however not adversely affected. It is a result of the flat-spring suspension of the magnetic wheels applying varying contact force on the soft rubber probe tires causing altered distance between the probe face and the backwall. A mode 1 measurement

technique is therefore not possible with this set-up. Instead, the thickness must be evaluated based on the time of flight between two back-wall echoes (mode 3) as shown in Figure 36.

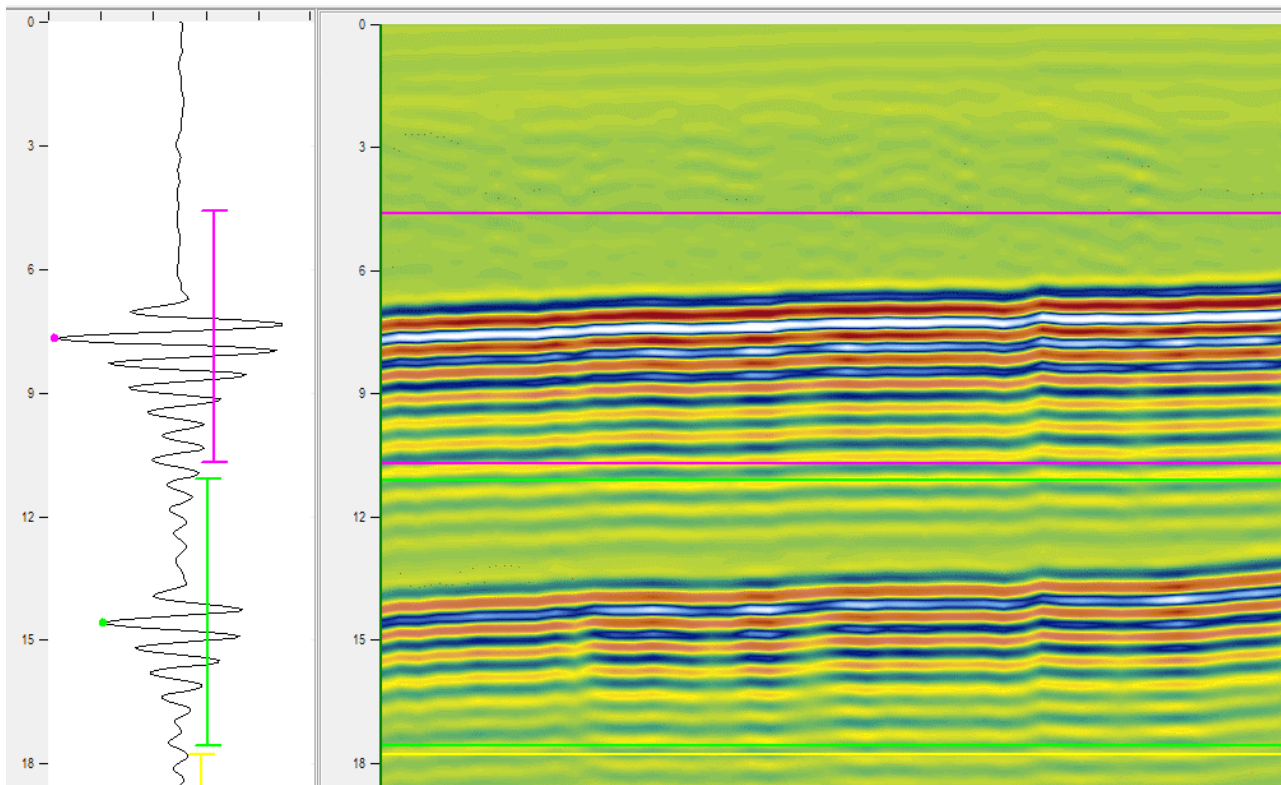


Figure 36: B-Scan of an 8-inch tube in longitudinal direction

3. Hybrid Robot with Arm

The HRA approach consists of a hybrid robot which can fly and crawl over the pipe while the inspection is being accomplished. This will be reached using a modular design of the aerial platform in which there are a main aerial system and different add-ons, which act as landing gear or ground system with different capabilities. Moreover, due to the demonstration and the final application of the system being focused on the inspection of pipes in oil and gas industry, the system has been designed with the possibility of entering into an emergency mode as follows: the aerial and ground subsystems can be separated, in a very short time, so that the aerial subsystem moves away along with the batteries and leaves the ground subsystem behind, guaranteeing safety conditions in the end user's facilities.

3.1. Modular Hybrid Robot Concept

The modularity of the HRA is one of its best advantages with respect to a conventional aerial platform. This system has been designed with a modular concept, so it can be adapted to the inspection scenario. The HRA system will be composed of three main parts, the aerial system, the magnetic linker and the different add-ons. The first two components (aerial system and magnetic linker) have been designed with transversal capabilities which do not depend on the application scenario (isolated pipes, racks, the need of movement capabilities...), whereas each add-on will be focused on one type of application with different capabilities. This allows improving the inspection performance through the selection of the proper add-on for each situation. Furthermore, the system could be easily extended in future

exploitation through the design of dedicated add-ons, which will improve the overall performance or will meet new requirements.

The scheme of this modular hybrid robot is presented in Figure 37 and Sections 3.2-3.4 will carefully explain the design result of each part.

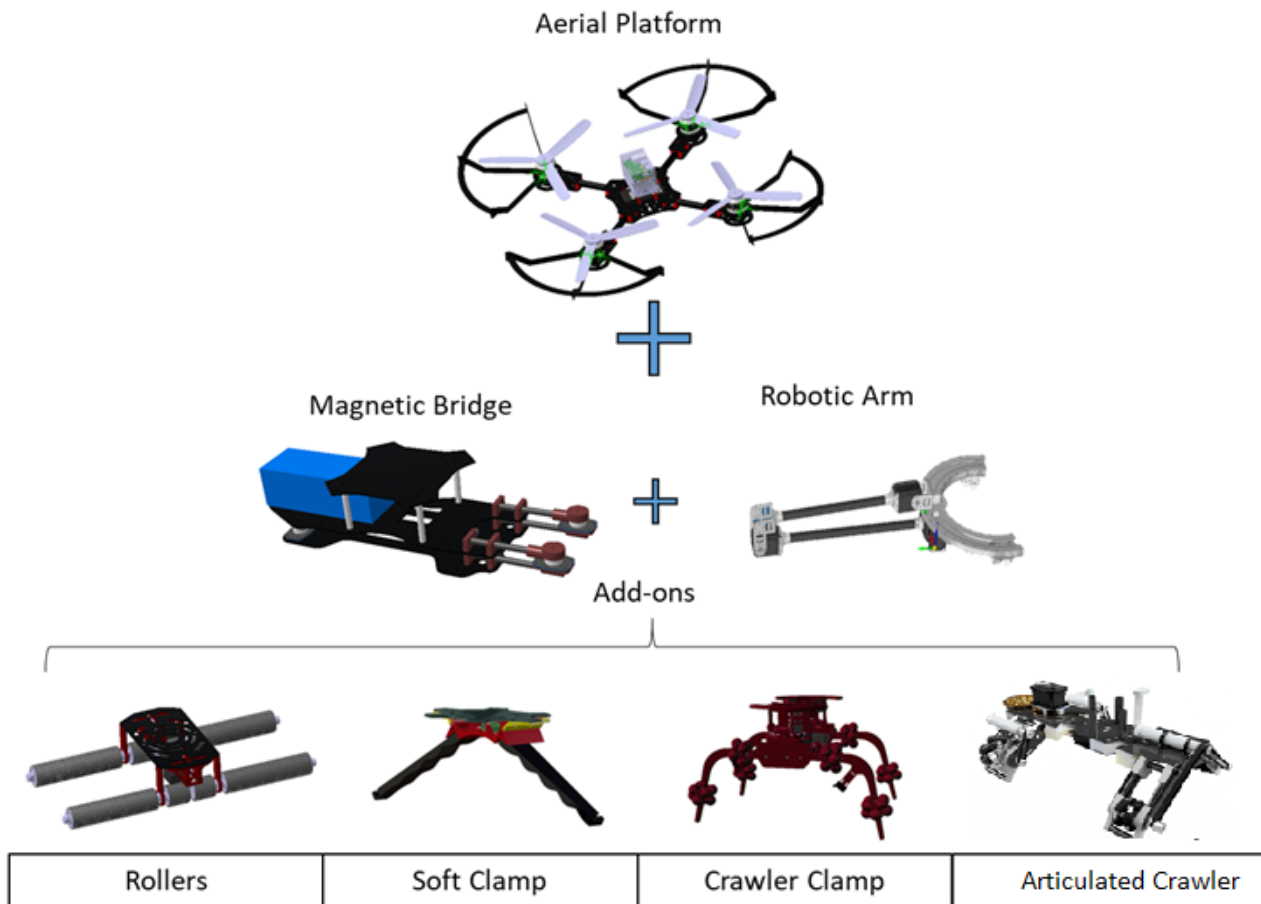


Figure 37: Modular Hybrid Robot Concept

3.2. Aerial Subsystem Details

The aerial system of the HRA has been designed to meet the end-users' and the application requirements while minimizing the size of the platform as much as possible. These requirements are:

- The aerial platform must be able to fly with the robotic arm and the inspection device.
- The landing gear must be able to accomplish a safe land over the pipe in autonomous or semiautonomous mode using a vision-based controller.
- The aerial platform must be stable over the pipe in safe conditions, and it must be able to crawl along it to reach different inspection points while it is landed.
- The propellers must be covered or protected to increase the safety conditions during the operation.
- In case of emergency, the aerial robot must leave the inspection area as soon as possible taking away the batteries and the sensitive equipment.

In order to meet these requirements, the first step of the design process consisted on approximating the mass distribution of the different subsystems demanded by the end-users and the applications

except for the aerial subsystem, because to define it, the mass and size details of the other subsystems are needed. This approximation was based on the previous results in other European projects and specific prototypes which have been developed during the first design stage of the HYFLIERS project. This approximation was:

Table 3. HRA first approach of mass system distribution.

Avionics System	
Autopilot	100 g
HLC	100 g
Inspection System	
Arm	1000 g
UT Sensor	200 g
Landing System (only one at the same time)	
Clamp	650 g
Rollers	650 g
Soft Clamp	650 g
Security System	
Magnetic Bridge	220 g
Propellers case	100 g
TOTAL	2270 g

Through this previous mass characterization, it is possible to estimate the size and the total weight of the platform which will be used in the HYFLIERS project. After several studies and iterations, the recommended size is a quadrotor platform with a diagonal between two opposite rotor axes of 620 mm. However, as the end-users emphasized in using an aerial platform as small as possible, we propose a smaller solution with a diagonal base of 500 mm, and which presents some limits to their requirements. Both platforms have the same layout but with different scale, as it is presented in Figure 38. From now on, the biggest solution proposed will be called the Full Requirement Robot (FRR) and the smallest the Limit Requirement Robot (LRR).

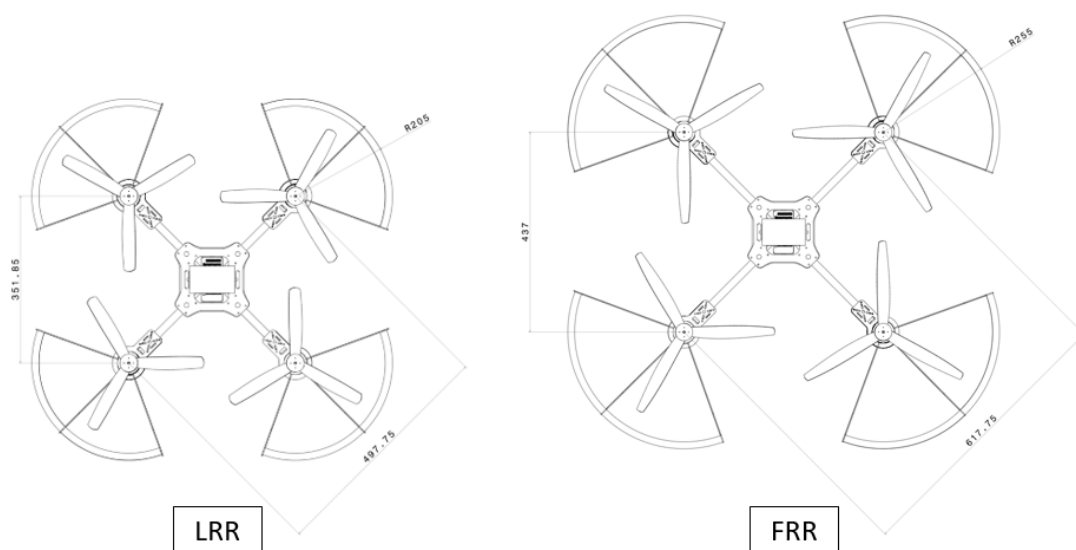


Figure 38: Layout and dimensions of the proposed solutions.

If it is assumed that the two main differences between the FR and the LR platform are the size and the motorization, the following subsections present a detailed description of the common parts of both aerial platforms proposed and the equipment onboard. It is needed to remark that the HRA is a modular platform and this section is only focused on the aerial mobility system and not on the ground part, so the details of the landing gear will be presented along the section dedicated to the description of the add-ons (Section 3.4).

3.2.1. Airframe Description

Due to the demanding requirements of the project, it was decided to develop a custom airframe minimizing the size and the weight of the aerial platform without lacking the structural strength and following the guidelines of the expertise obtained in previous projects.

The airframe designed is presented in Figure 39.



Figure 39: Airframe design

The chosen materials have been carbon fibre for the central plates, the motor stands and the tubes, and aluminium for the separators. The size of the central plate has been designed to fit the autopilot and the HLC in the upper part, along with the battery, where they are far enough of the landing gear and the magnetic bridge to avoid the magnetic interferences.

3.2.2. Avionics systems

Autopilot and HLC

As it was presented in the global system architecture in Section 1.3, the avionics will be composed of three main parts: the autopilot, which is in charge of running the main parts of the low level controller of the aerial system and the high level computer which has the functions of controlling and monitoring the mission and accomplishes the most complex parts related with the image processing or the task manager for the inspection device.

The autopilot solution used during the development phase in the HRA is the combination of a Raspberry Pi + Navio2 sensor shield. However, if it is possible and the final algorithms are light enough, we will use the common Pixhawk autopilot during the last phase of the project because it is a widely tested device which will allow us to increase the TRL during the final demonstrations.

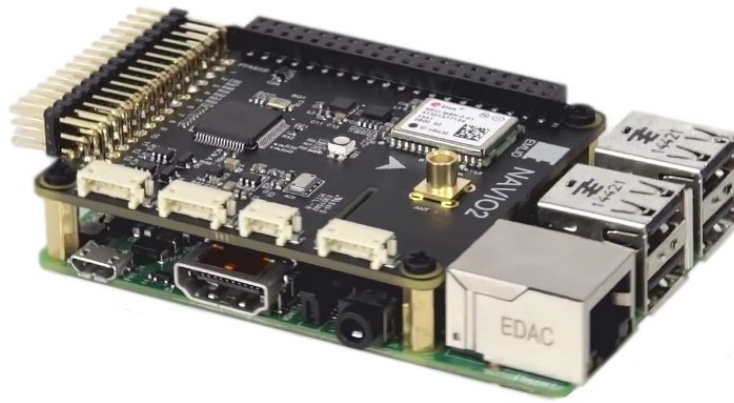


Figure 40: Raspberry Pi 2 Model B + Navio2

This autopilot has the following sensors in the Navio2 board that allow obtaining the status of the aircraft:

- A dual IMU, with a MPU9250 9DOF IMU and a LSM9DS1 9DOF IMU. Each IMU provides inertial data in three axes of accelerometers and gyroscopes. It also has measurements of the magnetic field in 3 axes which are used to determine the orientation of the aircraft.
- A MS5611 barometer for measuring the barometric height.
- An integrated U-blox M8N GLONASS/GPS/Beidou receiver with antenna connector type MCX.

The aerial robot also has a camera which will be used to carry out the vision algorithm to detect the landing target (a tube selected by an operator) and to feedback the controller during the vision-based landing manoeuvre.

The HLC will be an embedded computer, in this case, the choice is a Jetson TX2, as this board is able to run the vision algorithm, which is the most restrictive in terms of computation.

Radio link and communications system

The control system for the pilot has a radio link with S-FHSS (Frequency Hopping Spread Spectrum) modulation, which automatically changes the frequency of the communications to minimize the effect of interference, making the link more robust.

The transmission of the telemetry data or the video streaming to ground will be done through a datalink Ubiquiti R5AC-Lite in 5150-5875 MHz with a maximum transmitted power of 100mW, or otherwise using a wireless modem integrated into the HLC.

3.2.3. Payload

One important difference respect to the classical assumption is that in this case, the landing gear has been considered as payload. This is due to the modular design that allows the use of three different modules with different functions during the inspection task. The other subsystems considered as payload are the robotic arm for inspection and the magnetic bridge used to connect the different modules.

Although these subsystems have their own subsections 3.3, 3.4 and 3.6, an estimation of the masses has been previously presented in Table 3.

3.2.4. Motorization and power supply system

The final step in the aerial subsystem design is the choice of the motorization and the power supply system. Due to the two solutions presented in Figure 38, two motorizations have been proposed in order to meet the requirements. The estimated performance of both solutions is summarized in Table 4.

Table 4. HRA aerial motorization and power supply details and performance.

	KDE 4215XF-465	KDE 4213XF-360
Propeller	Triple- Blade: 12.5" x 4.3	Triple- Blade: 15.5" x 5.3
Mixed Flight Time	9 '	10.8 '
Maximum additional payload	1699 gr	3551 gr
Throttle	72%	63 %
Drive Weight	2893 gr	2805 gr
Estimated maximum temperature	45 °C	54 °C
Thrust-Weight	1.5	1.8
Battery	LiPo 10000mAh-25/50C	

3.2.5. Fault tolerance functions

Response to loss of GPS signal

If the GPS signal is lost during an autonomous or assisted flight operation using this type of positioning, the autopilot will immediately switch to attitude mode. If the GPS signal is recovered, if 2 seconds elapse without losing it again, then the autopilot will switch back to GPS mode. In the case in which the loss of GPS signal occurred when the aircraft flies in manual mode or attitude mode, the operation would not be affected since in these modes the GPS signal is not necessary.

Response to loss of communications

If the radio link control is lost for 3 seconds or more, the autopilot would automatically change to failsafe mode. In this case, the system is configured to perform a back-home maneuver. In the case of not having a GPS signal, the aircraft will not be able to perform this maneuver and will proceed to perform a stationary flight maneuver.

Battery level protection level

If the voltage of the flight batteries is below a pre-set limit, protection modes will be activated by low battery level. There are two levels of protection:

- The first low-level battery protection is activated when the voltage starts to be low, but there is still enough to maintain the manoeuvrability of the aircraft for a few minutes. In this case,

the aircraft will automatically make a manoeuvre back home. If a good GPS signal is not available, the system will be kept in stationary flight. The pilot will always be notified with an indicator at the control station.

- The second low battery protection is activated when the voltage level reaches a compromised level. In this case, the aircraft will proceed to perform a gradual descent manoeuvre. The pilot will be notified with an indicator at the control station.

In any case, during the pre-flight checks and during the flight, the battery voltage of the aircraft is periodically checked. During the planning of flights, care is taken to plan the flight in such a way that a margin of a couple of minutes of autonomy is available, in order not to reach a level of voltage close to the levels of protection.

The aerial robot also has two acoustic warnings that measure the voltage of each element of the battery and emit audible beeps when the cell level is below a threshold value set at 3.5 V to warn of the low level of the battery.

These protection modes may be varied depending on mission planning.

Lights installed

These flights are planned to be carried out under visual meteorological conditions (VMC), according to visual flight rules, between sunrise and sunset, with which this RPA is currently not provided with navigation lights.

3.3. Magnetic Bridge Description

The Magnetic Bridge is one of the main novelties included in the HRA. During the phase of specifications of the HYFLIERS project, end-users emphasised the need of including an emergency protocol to take-off from the pipe moving all the sensible parts like LiPo batteries away from the pipe as soon as possible. However, due to the characteristics of the robotic arm previously presented in the D1.2 and detailed in Section 3.6 of this report, the emergency protocol could be limited because the arm has to return to its home position and folded itself to take-off from the pipe. Thus, the final decision to meet the end user's requirements without changing the arm concept was to design a magnetic bridge which is able to detach the aerial system from the landing gear leaving it in the pipe with the robotic arm.

Therefore, this device acts as the common interface for attaching the add-ons and the robotic arm to the aerial platform and has two main functions:

- It is the core of the modular concept providing easy and fast interchangeability of the different add-ons.
- It provides the capability of remotely detaching the aerial subsystem from the add-on and robotic arm. Thus, the drone can leave the add-on and the arm, and quickly take off, carrying the batteries to a safe place during an emergency condition.

The Magnetic Bridge is composed of five permanent electromagnets distributed under the aerial platform, and five ferromagnetic targets fixed to each add-on (Figure 41).

The bottom plate of the drone (Figure 42) is a 2mm thickness carbon fibre plate which is fixed to the central plate by aluminium spacers. The bottom plate extends backwards to house the main battery on its rear side. Under this plate, three of the five electromagnets are screwed. On the front side, two carbon fibre tubes are fixed through clamps. Both tubes extend forwards, with the other two electromagnets placed in their end tips.

The top plate of each add-on (Figure 43, Figure 44 and Figure 45) is a 2mm thickness carbon fibre plate with mounting holes for the landing mechanism. Three of the five targets are screwed to the plate, aligned with the three electromagnets of the bottom plate of the aerial platform. On the front side, two carbon fibre tubes are clamped, extending forwards. The other two targets are attached to the end tips of these tubes, also aligned with the two frontal electromagnets.

The robotic arm is attached to the front side of each add-on, by fixing it to the two frontal carbon fibre tubes clamped to the top plate, so that, the arm's weight is distributed between the three frontal targets and electromagnets. This configuration is necessary to avoid torques that tend to separate the electromagnets from the targets.

The battery is placed in the rear side of the aerial platform to compensate the weight of the arm, attached to the front side.

Element	Dimensions (mm)
Frame bottom plate (without frontal tubes)	350x165
Frame bottom plate (with frontal tubes)	430x165
Frame bottom to centre plate separation	60
Bottom plate to add-on separation	15
Add-on plate dimensions (without frontal tubes)	300x165
Add-on plate dimensions (with frontal tubes)	388x165

Table 5. Magnetic Bridge dimensions.

Dimensions are subject to change, as the design must be adapted to the final dimensions and weight of the arm.

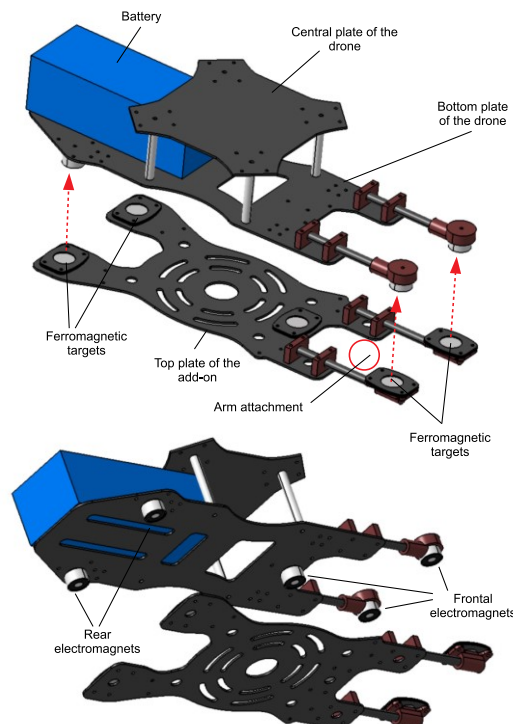


Figure 41: General view of the Magnetic Bridge.

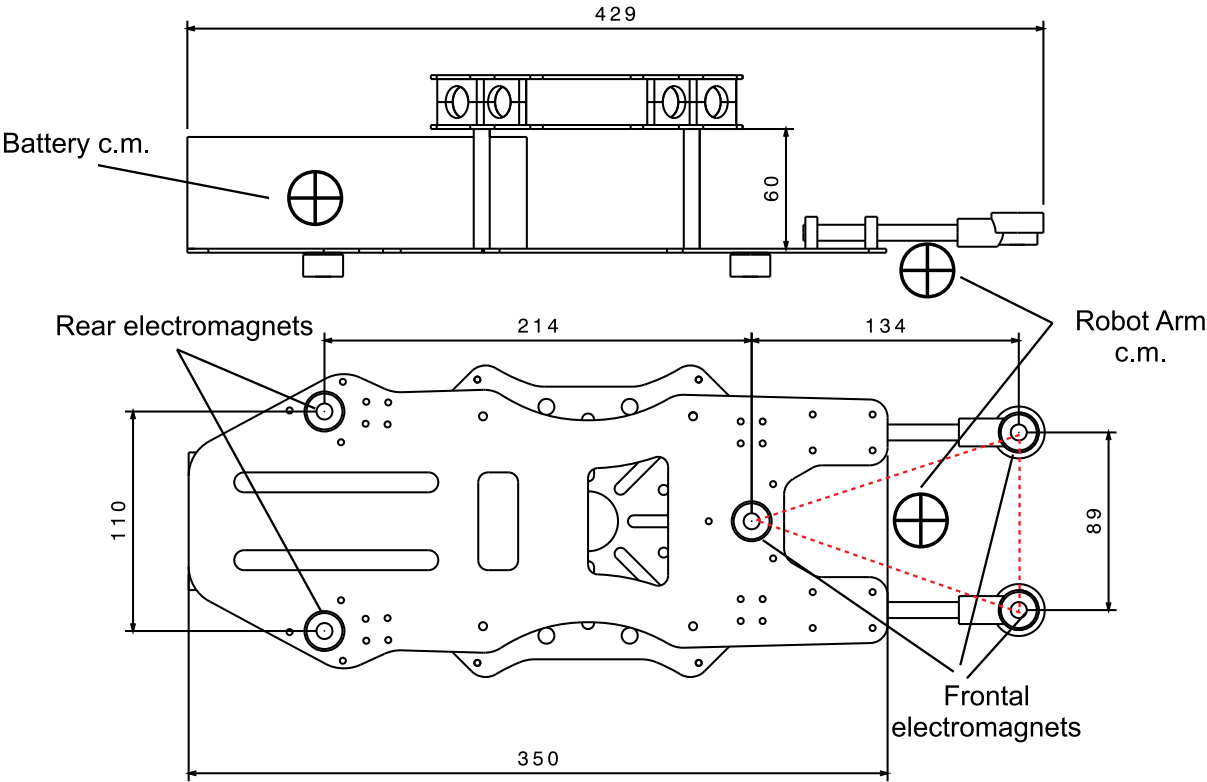


Figure 42. Dimensions of the bottom plate of the aerial platform.

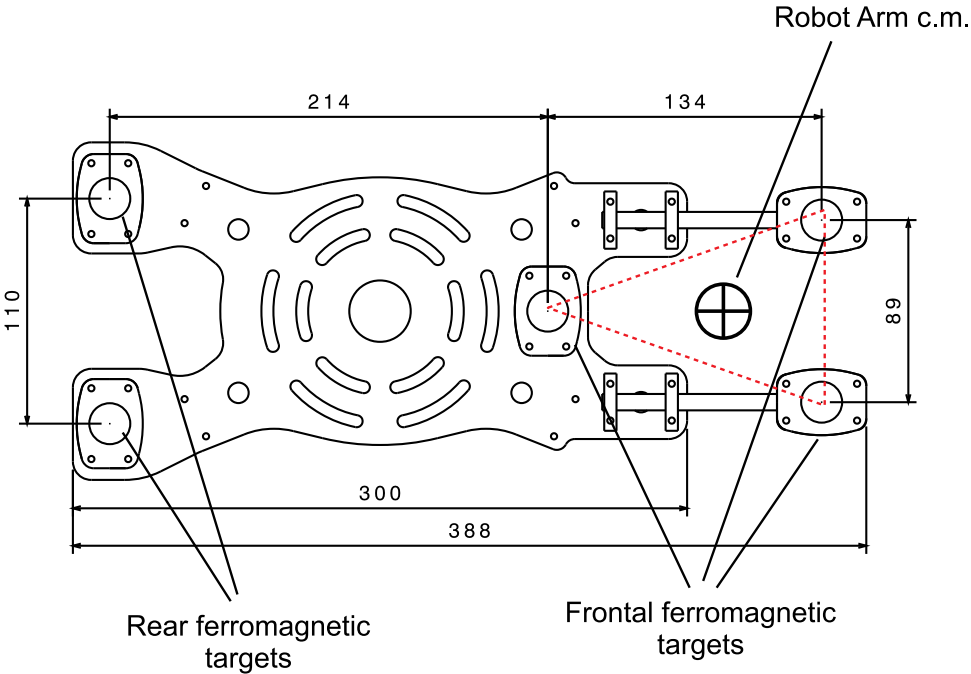


Figure 43. Dimensions of the top plate of the clamp add-on.

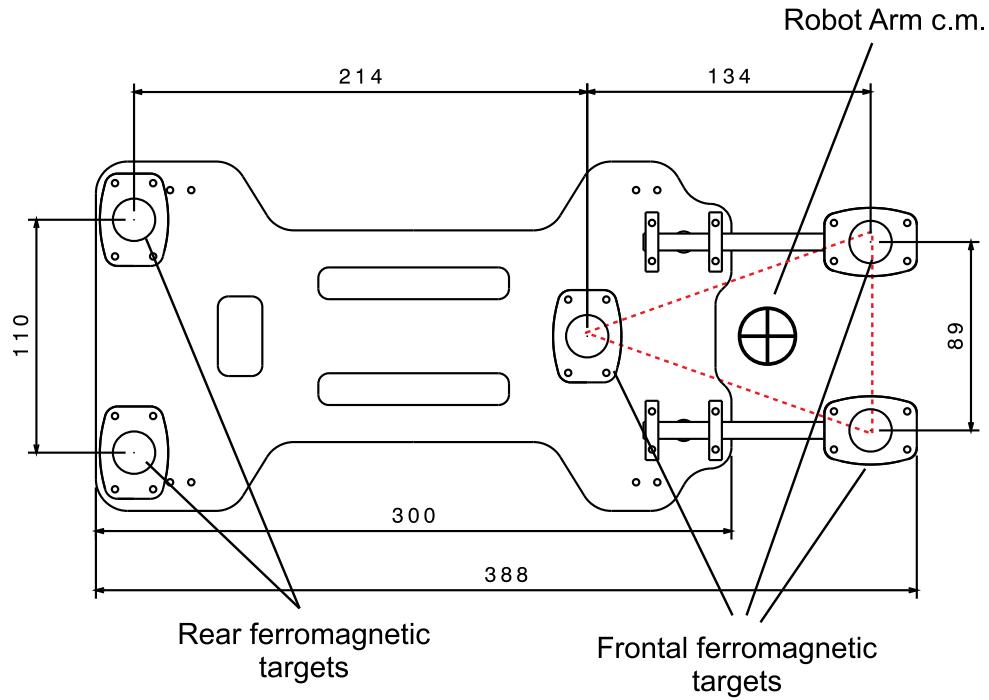


Figure 44. Dimensions of the top plate of the rollers add-on.

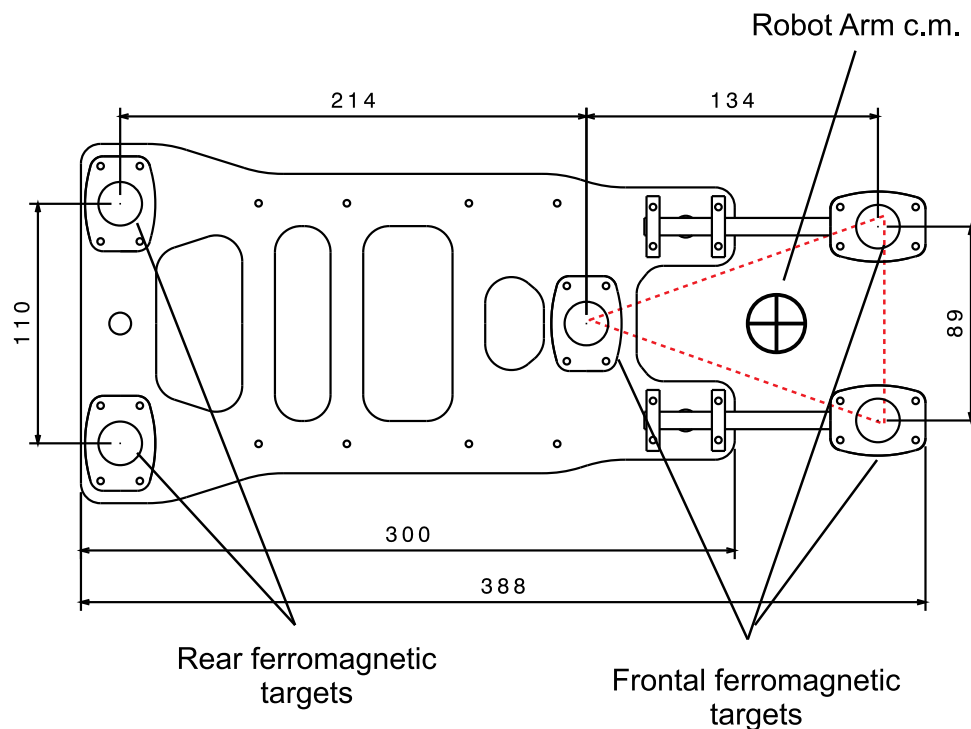


Figure 45. Dimensions of the top plate of the flexible clamp add-on.

The permanent electromagnets are 15mm height and 15mm in diameter (Figure 46). They can be screwed to the bottom plate of the aerial platform through an M4 screw. The targets are discs cut off a ferromagnetic metal plate between two carbon fibre plates, with screw holes for attaching to the bottom plate and clamps. The magnetic field is active while no power is supplied, generating an

adhesive force of 2.0 kg per piece. When a voltage of 24 V is applied, the magnetic field disables, with a consumption of 3.6 W per piece, and no pulling force is produced.

The permanent electromagnets can be powered by the 6S drone main batteries or by their own batteries. A microcontroller enables or disables them through a driver. In normal operation, permanent electromagnets are not powered, pulling the targets and keeping the add-on and the robotic arm attached to the aerial platform. In case of emergency, power is cut off, releasing the add-on and the robotic arm (Figure 47).

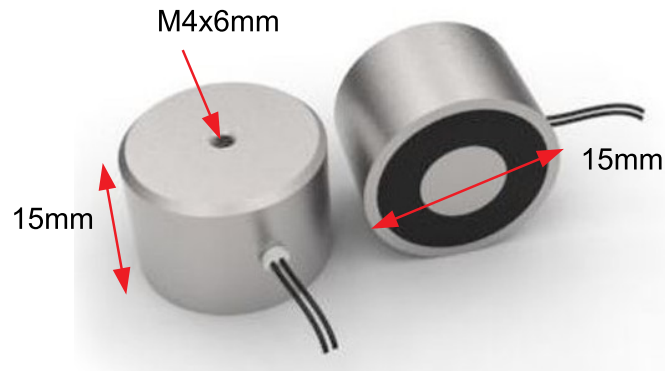


Figure 46. Permanent electromagnets.

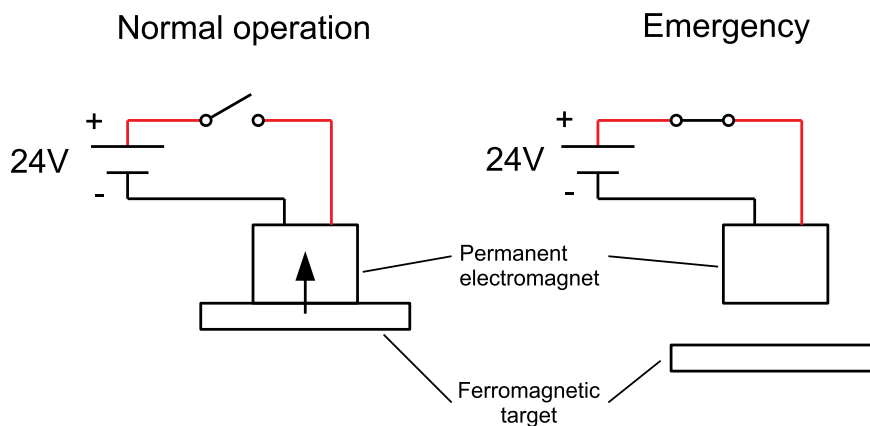


Figure 47. Operation of the permanent electromagnets of the Magnetic Bridge.

Element	Weight (g)
Electromagnets	100
Clamps and targets	160
Top add-on plates	80
Bottom drone plate	90
Carbon Fibre Tubes	50
Total	480

Table 6. Weights of the Magnetic Bridge elements.

The hardware is composed of a small microcontroller which activates or deactivates the magnet through a Pulse Width Modulation (PWM) signal. The microcontroller is directly connected to the onboard computer which commands it. A software library has been implemented to allow to operate the attaching system from either UAV's radio controller or the computer. The overall behavior of the attaching system software is shown in Figure 48.

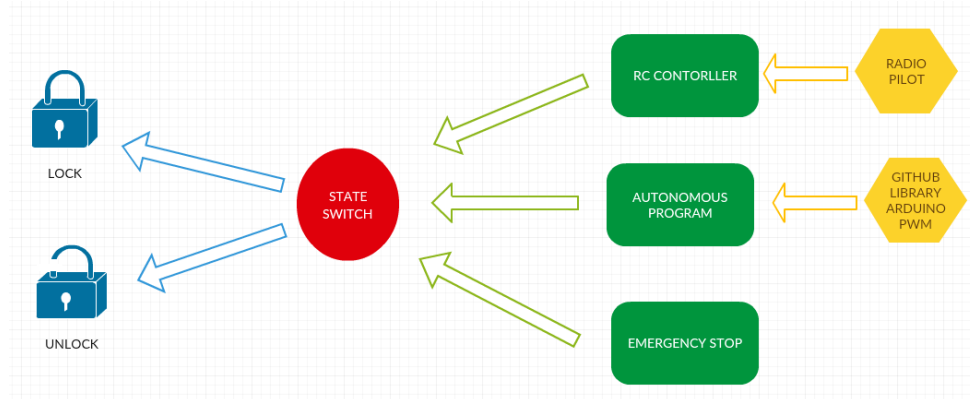


Figure 48 State diagram of the electromagnetic attaching system to exchange the add-ons.

3.4. Add-Ons Description

This section presents the different add-ons and their functionalities proposed for the HRA platform, it also presented a comparison in Table 7, where are shown the advantages and disadvantages of each add-on with respect to the others after a short description of them.

	Clamp	Soft Clamp	Rollers	Articulated Crawler
Linear movement over the pipe	X			X
Rotation passive movement	X			
Rotation active movement				X
Steering capabilities	X		X	X
Detachable emergency system	X	X	X	
Soft materials		X	X	
Passive docking		X	X	
Racks inspection			X	
Adaptability on pipes with different diameter	X	X		X

Table 7. Add-ons capabilities comparison.

The minimum and the maximum clearance between the pipes play a key role in design for an inspection operation. Figure 49 details the clearance limits for each add-on.

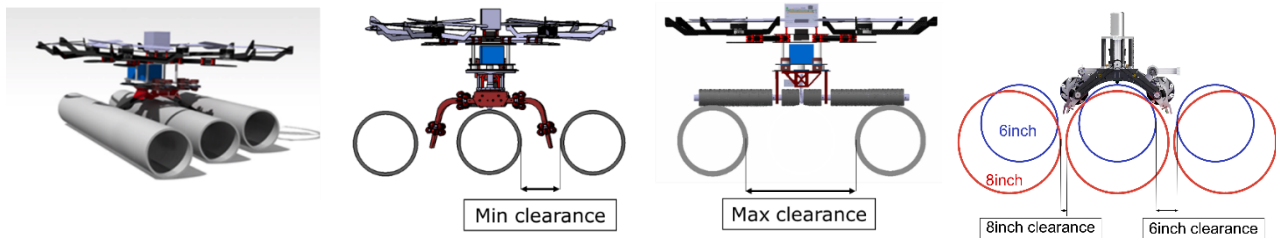


Figure 49 Clearance requirements for each add-on

3.4.1. Clamp Add-on

This add-on is designed to allow the aerial system to land over a single pipe (see Figure 50 and Figure 51), so it can perform inspections on isolated pipes. It consists of two pair of clamps which can be opened and closed simultaneously. The aerial platform approaches the pipe, and when about to land over the pipe, the clamp closes around it. This mechanism is capable of grasping pipes with different diameters.

Once over the pipe, the clamp does not restrict the movement. A set of omni-wheels on the clamp make possible to displace in the forward direction of the pipe and allow lateral movement over its circumference. The longitudinal displacement is controlled with a traction wheel, which consists of a continuous rotation servo plus a rubber wheel for better grip to the pipe. A shock absorber allows overcoming pipe joints and other minor obstacles over the pipe surface. The lateral displacement allows for stabilization in the case the platform does not land over the 12 o'clock of the pipe. In this case, the propulsion system laterally stabilizes the HR around the pipe.

The concept of a clamp with omni-wheels has previously been presented in this project, in the deliverable D1.2, and has already been tested over single isolated pipes where the crawler could displace over straight pipes. However, this concept was unable to displace over elbows. This is especially important, as elbows are important areas for inspection. To solve this problem, an ingenious yet rather simple mechanism has been designed.

The new clamp design adds a passive mechanism which makes it possible to overcome elbows Figure 51. It allows each clamp to freely turn, without the need of actuators, regardless of one to respect the other. During flight the mechanism is locked, so the clamp maintains a fixed position and doesn't disturb the flight. Once the aerial platform lands over the pipe, the weight of the platform over the crawler releases this elbow mechanism. The crawler displaces along the pipe as normal thanks to the traction wheel. If an elbow is reached, the crawler adapts to its curvature and keeps moving over the elbow. When over an elbow, the traction wheel direction is controlled with an additional servo, so it eases the turn by projecting the traction in the proper direction. The mechanism is passively locked again after taking off, as the weight of the aerial platform does no longer rest over the crawler.

To integrate and validate all these concepts, a first prototype is made of PLA additive manufacturing, which is suitable for fast prototyping. Once validated, ongoing prototypes will employ carbon fibre for weight reduction and higher resistance. Future designs will be focussed on reducing the number of pieces for ease of assembly and improving tolerances to reduce looseness and vibrations.

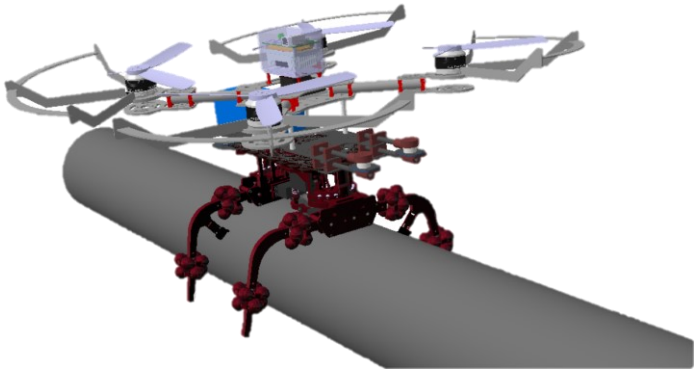


Figure 50 Clamp concept

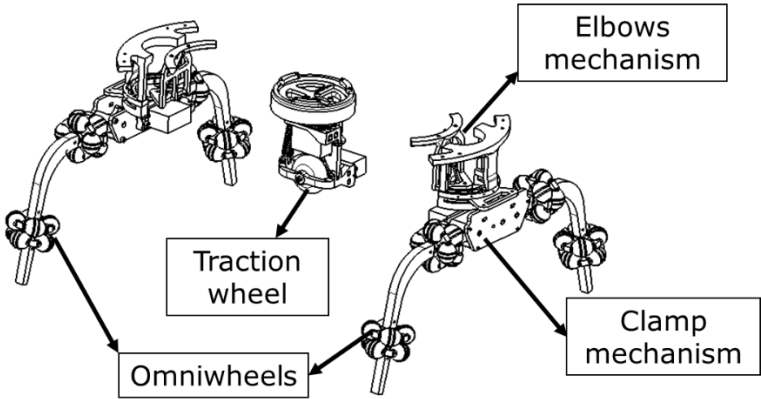


Figure 51 Clamp add-on main parts

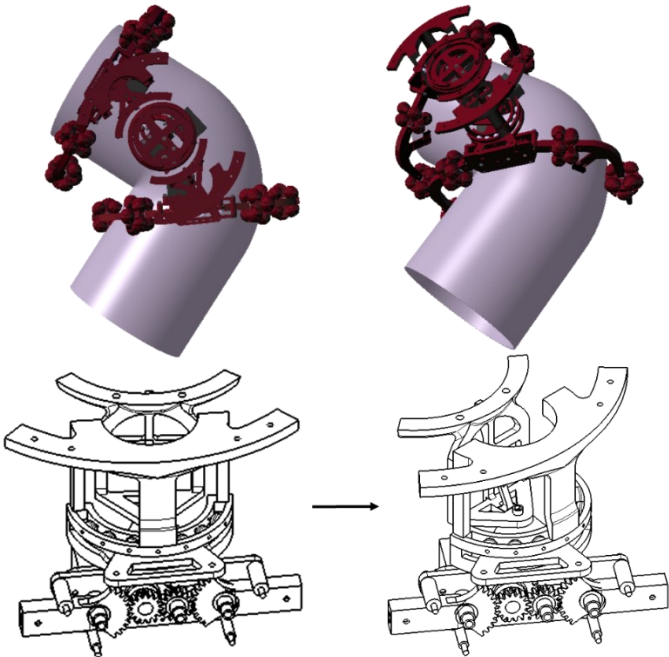


Figure 52 Passive elbow mechanism

3.4.2. Soft Clamp



Figure 53. Soft clamp – fixed Version.

This section describes a soft clamp module to attach the UAV robustly to the pipe during inspection and maintenance tasks. Two designs will be introduced, the first of them is a preliminary concept model used to strongly attach the UAV. The second design focuses on enabling this soft gripper to creep over the pipe, the UAV can move along the pipe while inspecting.

In both cases, the limbs are made in filaflex. This material is elastic and has great friction coefficient and softness. The principal advantage of using this material against other soft materials is that it can be used in additive manufacturing. Thus, it is possible to design a variety of models without restrictions that are typical of other manufacturing processes. Parts made in filaflex are rigid enough for keeping the shape, but also flexible to bend and adapt to the pipe's shape.

Soft Clamp – Fixed Version

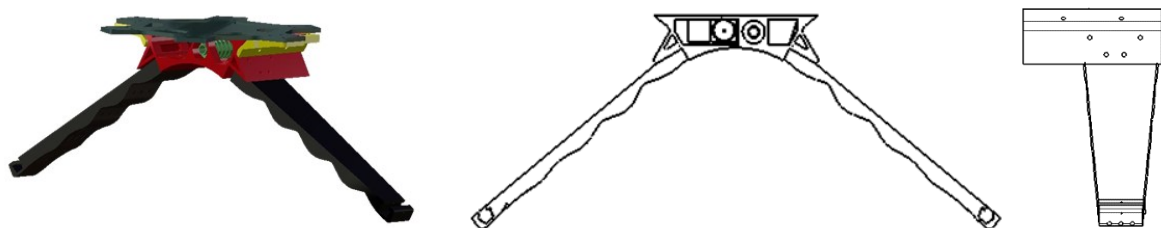


Figure 54. Fixed soft clamp design.

For the fixed landing gear, two limbs are used. These limbs have been carefully designed with special geometry and shape, that allows them to deform and adapt to a variety of pipe diameters and shapes. The top left image in Figure 46 shows the profile of the limbs, having different undulations and being more pronounced at the base and decreasing close to the tip. This design achieves greater deformations at the base of the limb to better adapt to the shape of the pipe.

The fixed soft-landing gear is composed of a rigid PLA chassis and two soft limbs that act like a claw. A servomotor is placed in the centre of the rigid chassis with a reel that pulls the different nylon threads to close and open the soft claw. The base of the chassis has been covered with silicone to increase the adherence and to enlarge the contact area between the pipe and the clamp. On the sides of the chassis are two soft limbs are placed. Each limb contains a reel that serves to roll up the nylon threads and, thus, bend the limbs. The end of this reel is inserted into a bearing in the opposite wall to reduce friction.

A design of the soft fixed landing gear has been developed during this period. The weight and the dimensions of the landing system are critical so that they have been optimized as much as possible obtaining a weight of 304.6 grams without the servomotor and 345.8 grams with the servomotor, having a dimension of 140 mm width and 96.5 mm height. The servomotor has dimensions of 40 x 20 x 40.5 mm, an operating voltage 6 - 8,4 V, a weight of 41 grams and a torque of 11.5 kg.cm. The advantages of this soft-landing gear are a great grip force, and it is very compact, achieving low weight and dimensions. Consequently, it allows better mobility in small spaces, and the soft material ensures that the pipeline is not damaged.

The choice of limbs shape has been obtained after looking for different nonlinear studies and tests, observing limbs' deformation and finding the best adaptive shape for the pipe. For those tests, the base of the limb was embedded, and a force was applied at the other end. This force was equal to the maximum force the threads would accomplish. Bottom images in Figure 46 shows example numerical tests performed for the optimization of limbs shape.

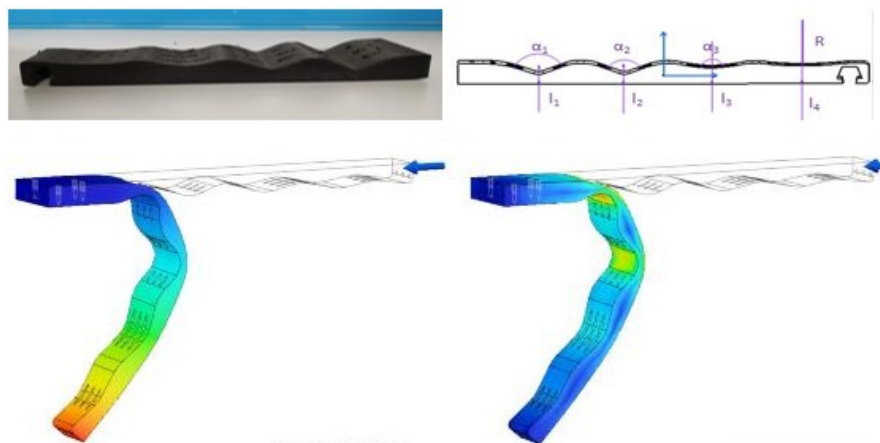


Figure 55 final limbs, displacement and stress analysis.

Each limb weights 36.9 grams, and they have dimensions of 52 mm width and 230 mm height. The maximum angle of grip to the pipe and the maximum slope to which it can be caught in the pipeline has been experimentally studied, obtaining for the first one a maximum angle of 35° degrees and a maximum slope of approximately 45° degrees. The final characteristics of the profile are shown in Table 8. l_1

Table 8 Limbs optimized angles and lengths

Angle	α_1	α_2	α_3	α_4
Degrees	132	135	166	170
Length	l_1	l_2	l_3	l_4
Millimetres	13	15	90	180

Soft Clamp – Mobile Version

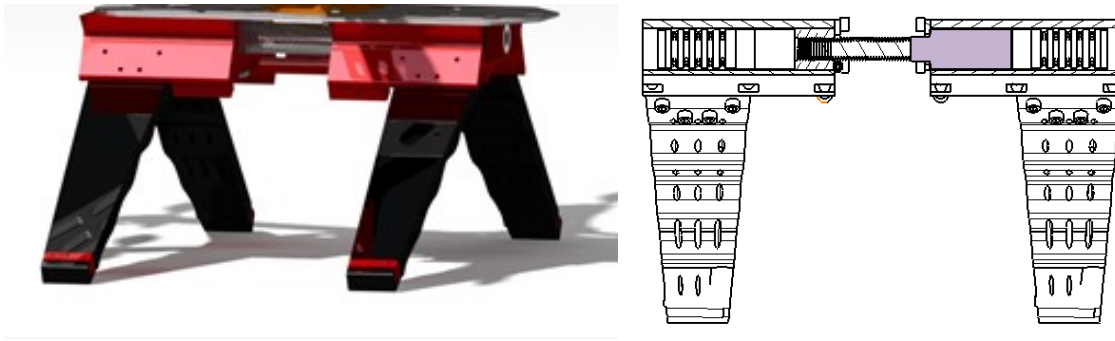


Figure 56 Mobile soft clamp system

The second design, i.e. the soft mobile landing gear, consists of a doubled clamp device that allows the UAV to move. Two symmetrical bases, one fixed and one mobile, located on the front and rear of the UAV are used to create this displacement. Each base has a pair of limbs that act as soft grippers.

The fixed base is joined to the frame through the connecting structure. It has two servos inside, one of them is responsible for operating the two soft limbs, with a reel that serves to roll up the nylon threads and bend the soft limbs to get the closure or opening, as same as the fixed version. The other servo is used to spin an endless screw that is connected to the symmetric base. In this way, the second base exerts a linear movement. From the top of the base, there are two metal bars to guide the mobile part of the mechanism. The bottom part of the base has a semicircular geometry to adapt better to the shape of the pipeline. Finally, there are several wheels that only move longitudinally at the ends of the base to facilitate the movement through the pipe and reduce friction.

The mobile base is identical to the fixed base, except for the fact that it only has one servo to move the second pair of soft limbs. The second servo is replaced by a nut that is fixed to the outer wall of the base where it relates to the endless screw. On the other side, it has two linear bearings in the upper part where the metallic bars of the fixed base will fit to allow a better sliding. In this way, it is possible to approach and separate bases using the smallest number of servos possible and optimizing the space and weight of the system. The same servos with the same characteristics as the fix soft land gear are used.

Moving along the pipe resembles a caterpillar' crawling. It is depicted in Figure 57 and it is described as follows:

1. In the initial position, the mobile base is in the closest position respect to the fixed base, and both pair of clamps are closed around the pipe.
2. For a forward (backwards) displacement, the pair of clamps belonging to the mobile (fixed) base is opened.
3. The servo connected to the endless screw starts to move:
 - 3.1 If the clamp of the mobile base was opened, it will advance until it reaches the top of the endless screw.
 - 3.2 If the clamp of the fixed part was opened, the whole platform will advance until the top of the endless screw is reached.
4. Once this point is reached, the endless screw servo stops, and the opened pair of limbs are closed. Now the mobile base is in the furthest position with respect to the fixed base.

5. To keep moving forward (backwards), the pair of clamps belonging to the fixed (mobile) base is opened.
6. The servo connected to the endless screw starts to move in the opposite direction described in 3:
 - 6.1 If the clamp of the fixed base was opened, the whole platform will advance until it reaches the mobile base.
 - 6.2 If the clamp of the mobile base was opened, it will advance until it reaches the fixed base.
7. Once this point is reached, the endless screw servo stops, and the opened pair of limbs are closed. Now the mobile base is in the closest position respect to the fixed base, as same as described in step 1.

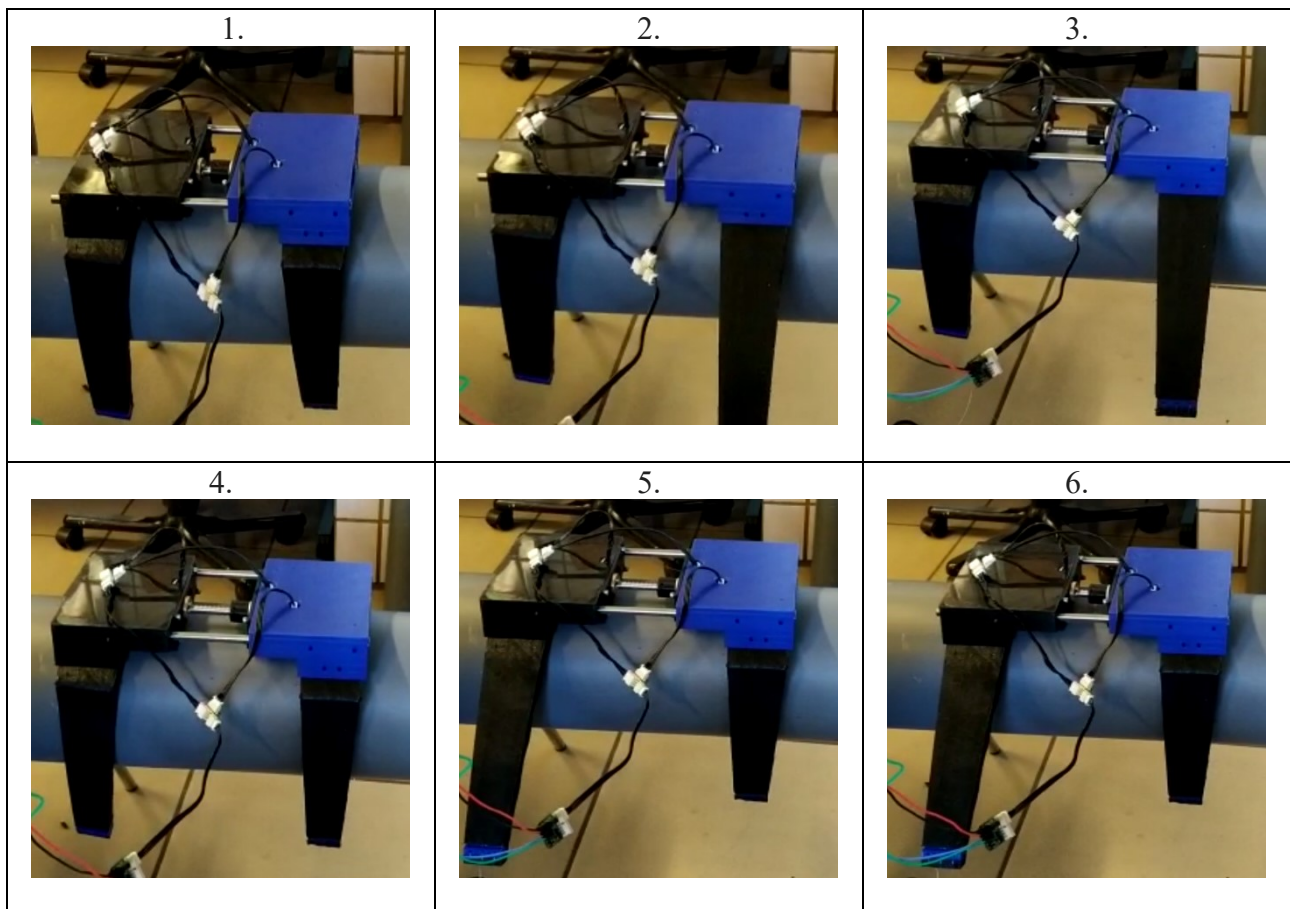


Figure 57 Soft mobile landing gear moving over a pipe.

Flight experiments have been carried out by landing on the pipeline with the soft fixed land gear, all the experiment have been performed outdoors, and in various weather and wind conditions, for this purpose, a test bench has been built with a shaped structure with 15-inch PVC.

Table 9 Specifications of two designs of soft clamp system

	FIXED SOFT LANDING GEAR	MOBILE SOFT LANDING GEAR
ANGLE (°)	35	--
STRENGTH (N·CM)	112.6	112.6x2
WEIGHT (MM)	304	800
WIDTH (MM)	140	290
HEIGHT (MM)	96.5	96.5
MAX SLOPE (°)	45	--



Figure 58 Sequence of autonomous landing using a soft clamp. It can be observed that the gripper has enough strength to pull the UAV towards the pipe to stick to it.

3.4.3. Rollers add-on (racks)

The requirements of the project contemplate the need to develop an add-on that allows inspections in pipe racks. Under this consideration, a landing gear made up of two rollers is carried out. In this way, the HRA can lean on two or more pipes. The number of pipes on which HRA can move will depend on the size and separation of the same. Figure 59 shows the design of the landing gear with the rollers.

The actual arrangement of the rollers on the pipe implicitly has several advantages:

- This configuration allows passive docking. After landing, the propulsion system can be turned off and the rollers can move along the pipes to perform the inspection.
- The design is intrinsically stable and does not need stabilization control
- Greater precision in handling.
- The landing procedure is simpler because the alignment of the rollers with the pipe is easily done.

The following figure shows the design of the landing gear with the rollers.



Figure 59 Rollers add-on and exploded view.

This landing gear consists of two rollers that can rotate and crawl over several pipes. The rollers move by a gear system placed in the central zone. These gears are powered by a continuous rotation servo. This design has a single motor which has been tested and proved to move a platform of up to 10 kg.

This add-on is made of different plastic parts, a carbon fibre shaft for each roller, four bearings, a continuous rotation servo, and a carbon fibre plate where the magnetic linker is mounted. The rollers are attached to the carbon fibre plate by two columns made of plastic. In addition, bearings are installed to ease the rotation of the rollers.

In order to minimize weight, the rollers are made of filaflex, the same flexible material as the soft clamp, so they can adapt to different pipe diameters and separations. Table 10 presents a first approach of the rollers add-on mass distribution. Furthermore, the rollers have been designed with certain roughness, like car tires, to provide sufficient friction force when they are in contact with the pipes.

Element	Weight (g)
Rollers	300 x 2
Motorization	100
Total	700

Table 10 Roller add-on mass distribution

The separation between the rollers is 220 mm. The length of each roller is 600 mm, and its weight is approximately 300 g. The motorization has a weight of 100 g. Therefore, the total weight is 700 g. The integration of the landing gear with the aerial platform and the magnetic linker can be seen in Figure 60.

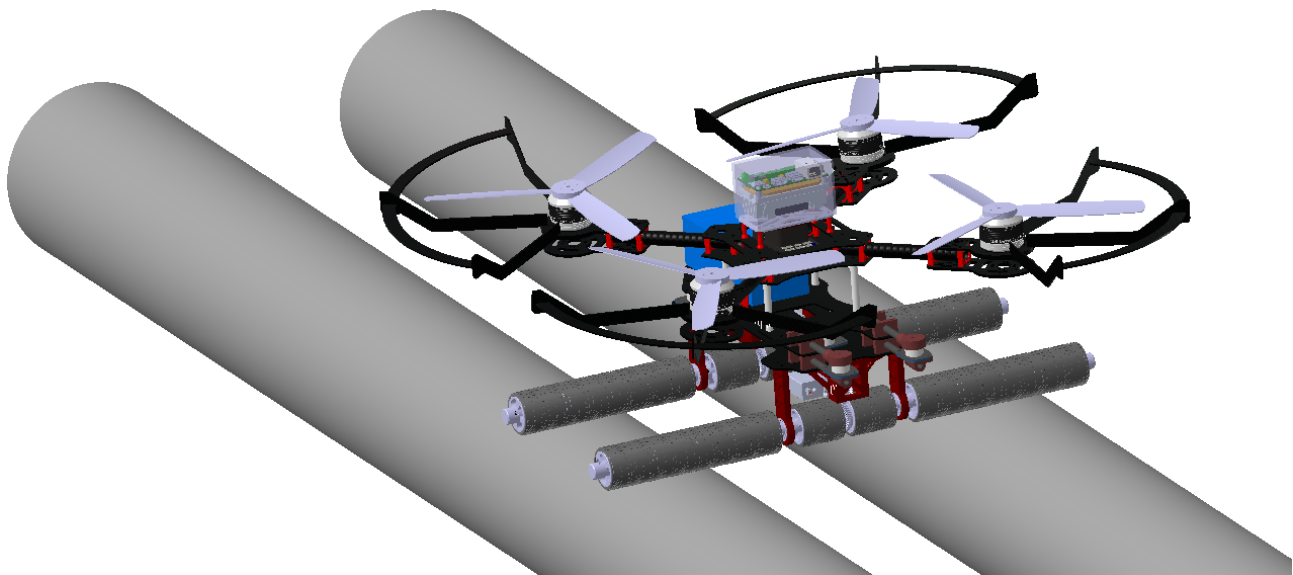


Figure 60 Rollers add-on concept.

3.4.4. Articulated rover

A novel patent-pending vehicle has been designed. The vehicle can walk on rectilinear and curved pipes thanks to its 2 DoF articulation. Moreover, the rover can auto stabilize itself on the pipe using wheels and propellers and thanks to the novel designed kinematics. Furthermore, we planned to use the rover also in combination with the ARAP180 and ARAP90, as it is possible to see in sections 3.4.3 and 3.4.4.

The wheel position and the rover structure have been designed to be adaptable to pipe with different diameters. In details, we are building a prototype able to walk on pipes with diameter in the range [6, 10] inches, that are the most common in a refinery.

Moreover, we developed the rover to be articulated using two revolute joints. The two actuated articulations are designed to allow the rover to move along the pipe standard curve (curvature ratio of 1.5D).

We used a total of three gear-motors to actuate the four wheels (two for the Meccanum-wheels and one coupled for the Omni-wheels). Maxon gear motors with a gear ratio of 1:103, a maximum torque of 0.8Nm and provided with encoders have been chosen.

Moreover, in this first prototype, the two joints are actuated using two Actuonix linear motors (<https://www.actuonix.com/>) with a linear displacement of 20 mm. This translates into a maximum angular displacement of the two joints in the range $[-30, 30]$ deg. Four laser distance sensors have been adopted to control the joints position to control the rover movement along pipes curve.

The articulated rover weight is approximately 750 g.

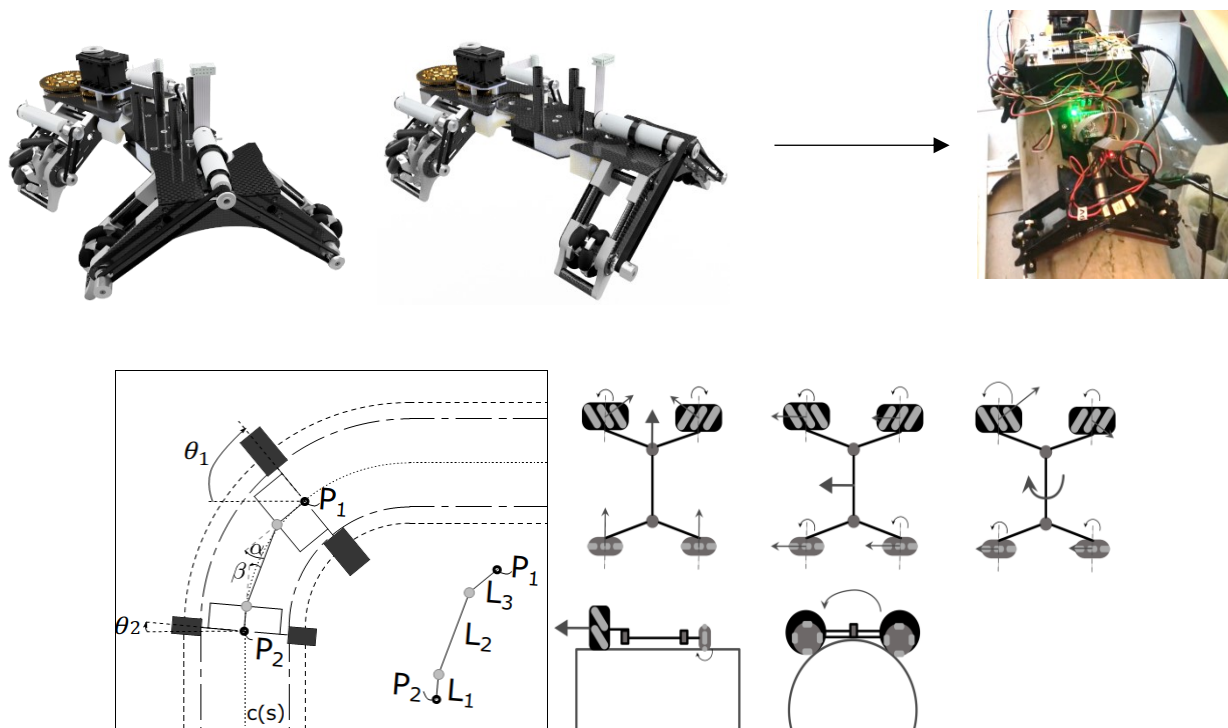


Figure 61 Articulated rover concept and proof of concept

3.5. HRA Stabilisation System using Propellers with Variable Pitch

The conventional multirotor design uses fixed-pitch propellers mainly due to their simpler mechanisms and easier control when compared with variable-pitch propellers. In the case of operation on the pipe with some grip mechanism, like magnets, the fixed-pitch solution seems to be suitable because its control, while operating on the pipe, is reduced to switch the magnet and this is the case of the HRA. On the other hand, when the design does not have a grip mechanism the variable-pitch solution becomes the only suitable one, because its ability to generate negative thrust (unlike the

fixed-pitch one) becomes necessary to keep the multirotor position under circumstances such as inaccurate landing position due to wind disturbances or clearance for the gripper.

Figure 62 shows the HRA(a) and a variable-pitch propeller (b). The dynamics of the multirotor on the pipe can be described as a 2-DoF radial and rotational motion $\{r(t), \theta(t)\}$, in direction of a line between centre of pipe and centre-of-mass (CoM) of the multirotor. Figure 62(a) the motion is depicted in XZ plane; (b) the linear motion of the central rod changes the angle of the blade while the rotor is rotating. The whole motion is also limited by the clearance of the clamp around the pipe.

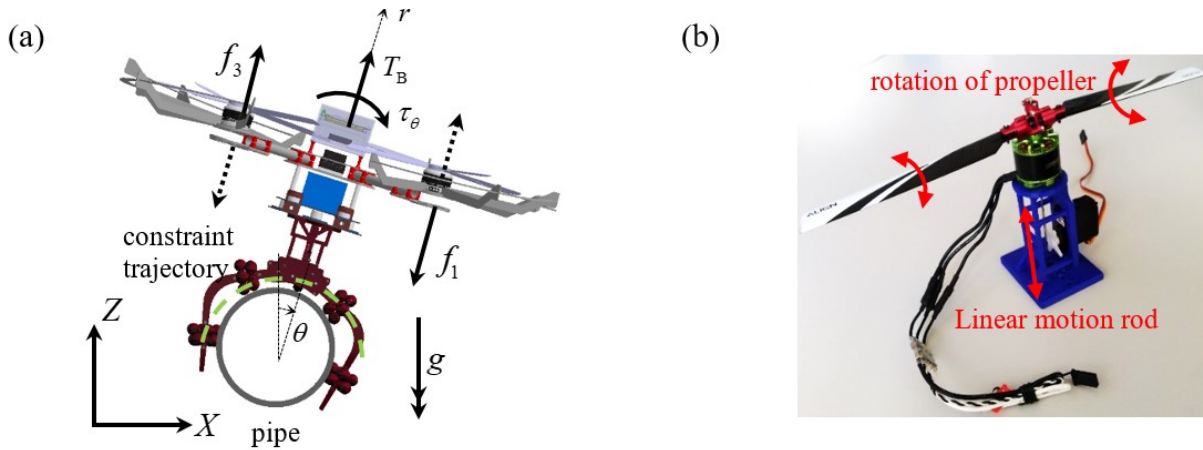


Figure 62(a) Multirotor on a pipe, 2-DoF rotating; (b) propeller with the variable pitch

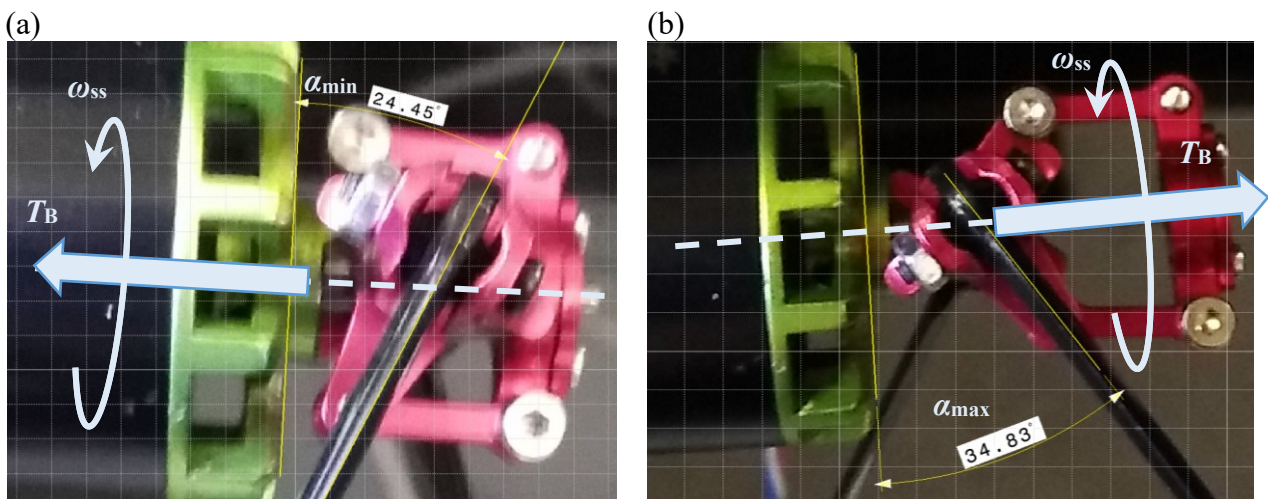


Figure 63. (a) Variable pitch propeller at minimum angle of the blade position; (b) maximum position.

The direction of thrust changes by variation of the angle of the blade between minimum and maximum range of $a \in [24.45^\circ, 34.83^\circ]$, Figure 63 (a) and (b), to produce a variable thrust force at a constant angular velocity of rotor ω_{ss} . The time response of the blade angle is very short, providing agile manoeuvrability. The change in the thrust is also highlighted in Figure 63. The blade angle was changed from minimum position -24.45 degrees to the maximum value, 34.83 degrees. The thrust increases accordingly by blade angle, from negative zone to positive one. The range for rotor angular velocity was $\omega \in [620, 1240]$ (rad/s).

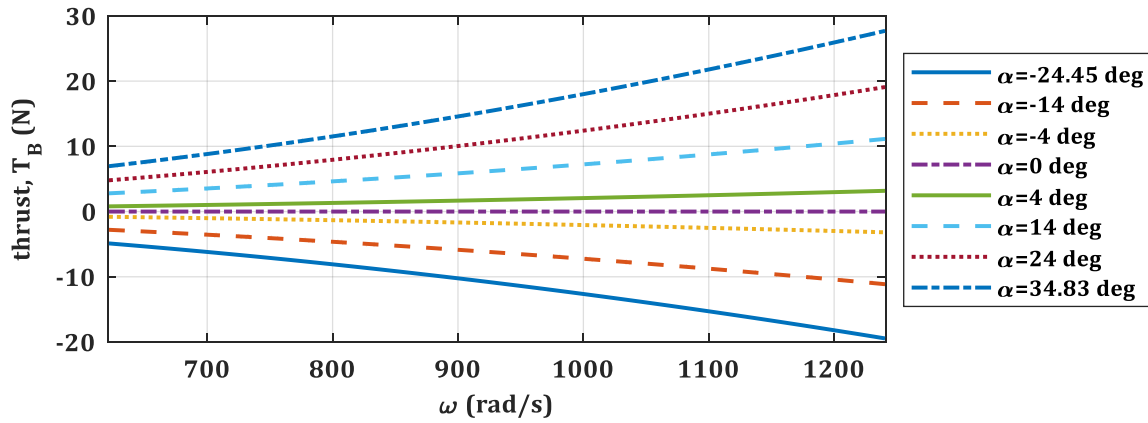


Figure 64. Thrust versus rotor angular velocity.

For the sake of comparison, let recall below the control allocation of the fixed-pitch propeller

$$\begin{bmatrix} \omega_1(t) \\ \omega_2(t) \end{bmatrix} = \sqrt{\begin{bmatrix} k & k \\ -lk & lk \end{bmatrix}^{-1} \begin{bmatrix} T_B(t) \\ \tau_\theta(t) \end{bmatrix}},$$

in which l (m) is a distance between rotor and CoM, k (Ns²/rad²) is the thrust factor and $\omega_i(t)$ (rad/s) is the angular velocity of the i -th rotor. Notice that this case is limited to one size rotation of the rotor, implying that the propeller can only generate positive thrust. On the other hand, the propellers with variable pitch possess the advantage of providing both negative and positive thrusts. Thus allowing, more manoeuvrability, upright or inverted flight, detach/attach equipment in out of reach positions and negative thrust deceleration among others [5][6]. [7] presents a control system for a quadrotor with variable propellers. The challenges are also complexity in rotor mechanism design, control approach and reducing the flight stability of the multirotor, but at the expense of an allocation scheme more involved. In particular, the thruster allocation can be defined in terms of thrust coefficient as in [8], and becomes:

$$\begin{bmatrix} C_{T,1}(t) \\ C_{T,2}(t) \end{bmatrix} = \begin{bmatrix} \gamma K & \gamma K \\ -\gamma l K & \gamma l K \end{bmatrix}^{-1} \begin{bmatrix} T_B(t) \\ \tau_\theta(t) \end{bmatrix}, \quad \alpha_i(t) = \frac{6C_{T_i}(t)}{\sigma C_{l_\alpha}} + \frac{3}{2} \sqrt{\frac{C_{T_i}(t)}{2}},$$

where γ is 1 for normal flight and -1 for inverted flight and $K = \rho \pi R^4 \omega_{ss}^2$ in which ρ (kg/m³) is air density and ω_{ss} (rad/s) is the nominal angular velocity of the rotors; α_i and C_{T_i} are blade angle and thrust coefficient of i -th rotor, C_{l_α} is aerofoil lift curve slope, $\sigma = N_b c / (\pi R)$ in which N_b is the number of the blades of each rotor, c (m) is rotor's chord length and R (m) is the radius of the rotor. Notice the additional DoF with respect to fixed pitch of varying $\omega(t)$ (positive and negative), providing much more manoeuvrability. To simplify the description, it has been considered at its nominal value ω_{ss} . This first prototype has $R = 140$ mm and nominal $\omega_{ss} \square 900$ (rad/s).

To show the advantages, a couple of simulations has been carried out. A 2-DoF model on a pipe under a wind gust (vanishing disturbance) deviated from the top desired position and closing the loop with a standard LQR-type cascade controller. In Figure 65(a) the wind gust provides a force/weight ratio >1 making that the fixed-pitch one fails under its impossibility of generating a counteracting negative thrust. In Figure 65(b) with the force/weight ratio <1 the fixed-pitch one was able to recover but, it

was forced to an undesirable excursion. However, in both cases the variable-pitch one succeeded in reaching the target near the pipe, overcoming such disturbance.

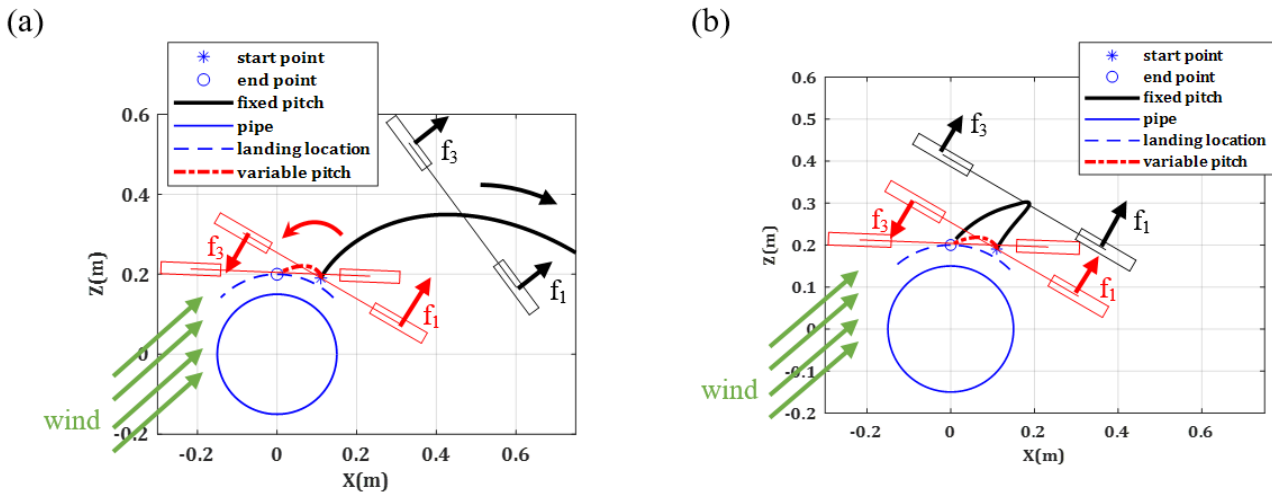


Figure 65 Performance of fixed and variable pitch in stabilisation.

In summary, the variable-pitch design can go to a negative thrust regime by changing the angle of the blades, and so it is able to compensate disturbances. Moreover, this design generates torque $\Delta f = f_1 - f_3$ (N) without any contribution to the total thrust, unlike the fixed-pitch design that generates a total thrust while producing torque. This latter characteristic emphasizes that the variable-pitch design also consumes less energy to balance the system.

3.6. Robotic-Arm Description

As discussed with the project partners and with the end-users we choose to develop different solutions for the HYFLIERS robotic arm at different TRL. The solutions will be presented with increasing level of complexity that translates to an increasing level of dexterity. In this task we summarize only the main aspects and capabilities of the different solutions, more details are described in the deliverable D3.1 [9].

3.6.1. Fixed Articulation with 180° Probe (FAP180)

The FAP180 prototype has been designed to observe the following requirements:

- Reduced weight respect to the other solutions to maximise the flight time and at the same time reduce the drone dimensions and weight.
- A simple folding solution of the sensorized end-effector allowing take-off and landing.
- Simple mechanics and control to reduce failure risks.
- Possibility to execute measures along linear pipes but also horizontal and vertical upward curves.

Based on the requirements the FAP180 is composed by:

1. A novel kinematic composed by a revolute joint and a driving guide.
2. A measurement tool able to rotate around the pipe axis about 180 degrees to move the instruments along its circumference.

The FAP180 needs to be mounted on an articulated mobile vehicle able to crawl on pipes as shown in the following figures (Figure 66 and Figure 67).

Tech specs:

- Arm weight 200g
- Tool weight 530g
- Permitted tool rotation: 180 degrees
- Number of UT sensors: 2
- Number of DoFs: 3



Figure 66 FAP180 design concept

In Figure 67 some use cases are reported. From the left to the right: measurement along linear pipes, measurement along vertical curves, measurement along horizontal curves.

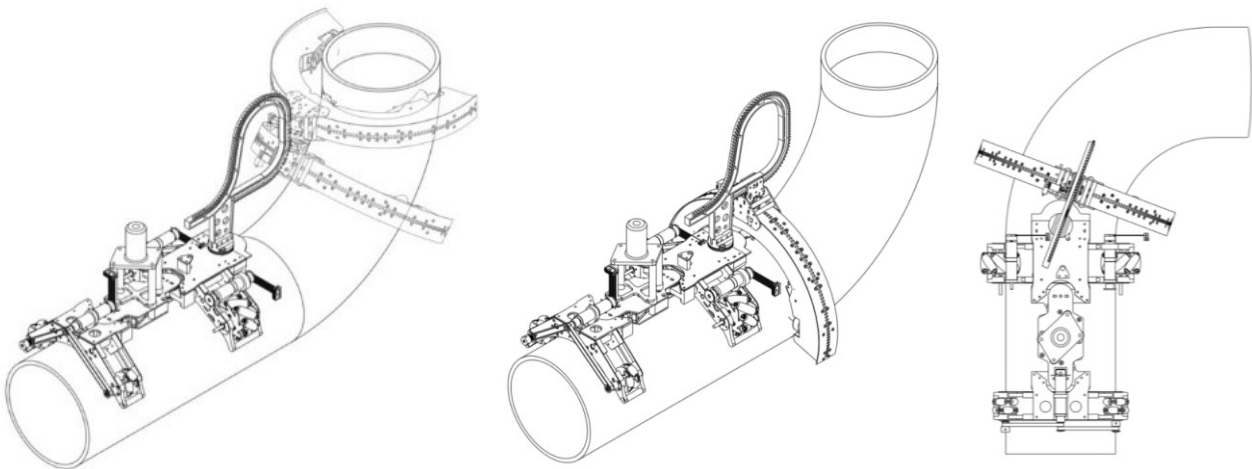


Figure 67 FAP 180 use cases

The drone vehicle frame will be attached over the central element of the articulated mobile vehicle.

3.6.2. Anthropomorphic Robotic Arm with 180° Probe (ARAP180)

The ARAP180 prototype has been designed to improve the FAP180 by enhancing system flexibility. In details, the ARAP180 is composed by:

1. An anthropomorphic robotic ARM with 5 DOFs
2. A measurement tool able to rotate around the pipe axis about 180 degrees to move the instruments along its circumference.

The FAP180 need to be mounted on an articulated vehicle able to walk on pipes as shown in the (Figure 68 and Figure 69).

Tech specs:

- Arm weight 750 g
- Tool weight 530 g
- Arm payload: 670 g
- Permitted tool rotation: 180 degrees
- Number of UT sensors: 2
- Number of DoFs: 5+1

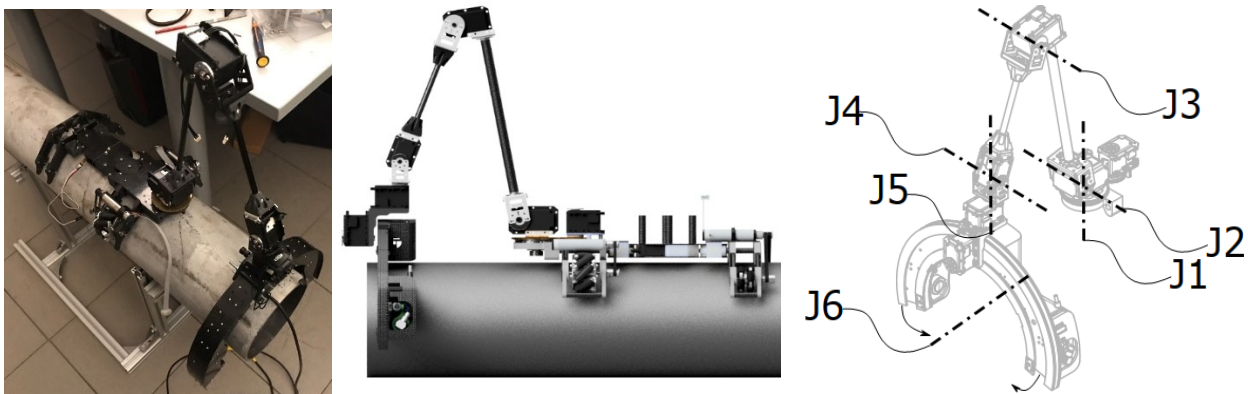


Figure 68 ARAP180 design concept and proof of concept

Thanks to the anthropomorphic arm the ARAP180 can perform measures along linear pipes, horizontal and vertical curves (upward and backward) and is also able to measure adjacent pipes.

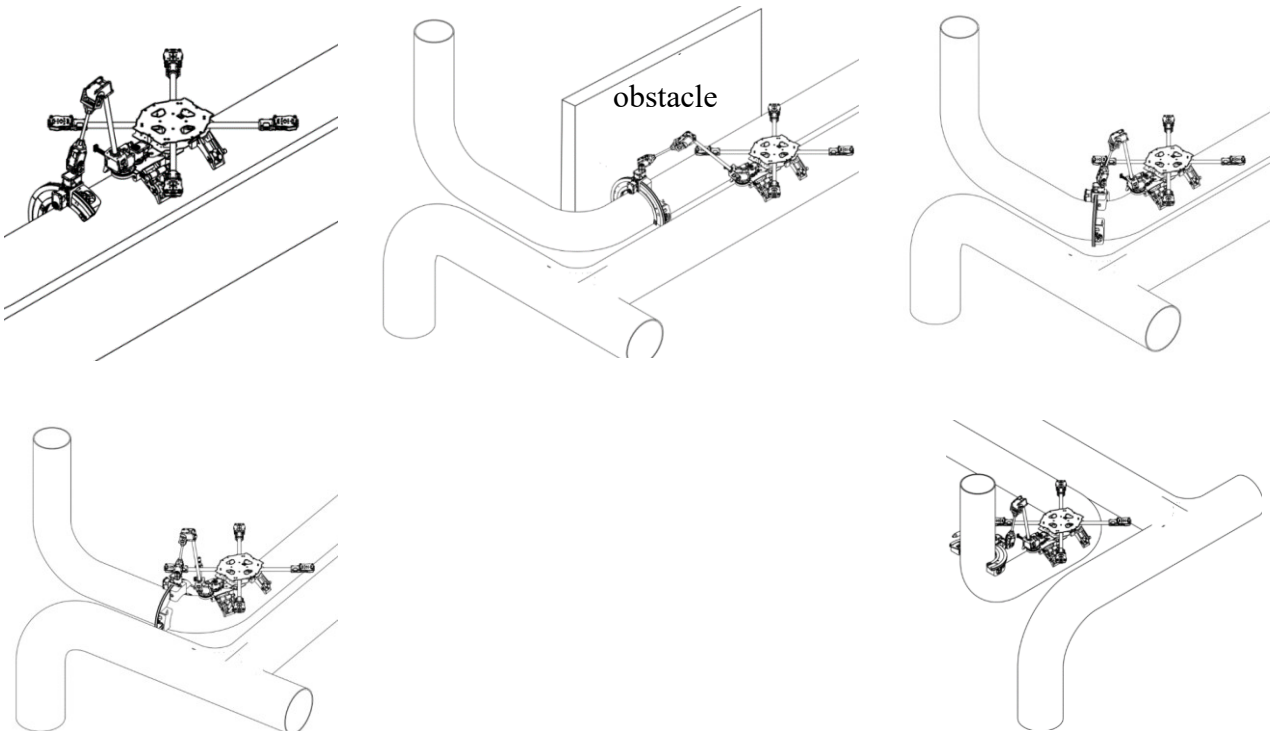


Figure 69 ARAP180 use cases

3.6.3. Anthropomorphic Robotic Arm with 90° Probe (ARAP90)

Another version of the ARA arm is the ARA90 that mount a 90-degree probe with a single UT sensor. This solution allows the reduction of the tool weight and at the same time increasing flexibility during measurements, also for **T sections**, Figure 70. However, to move this tool the arm requires an additional DoF in the wrist, for a total of 6 DoF in the arm and one DoF more internal in the tool, to reach all measurement configuration.

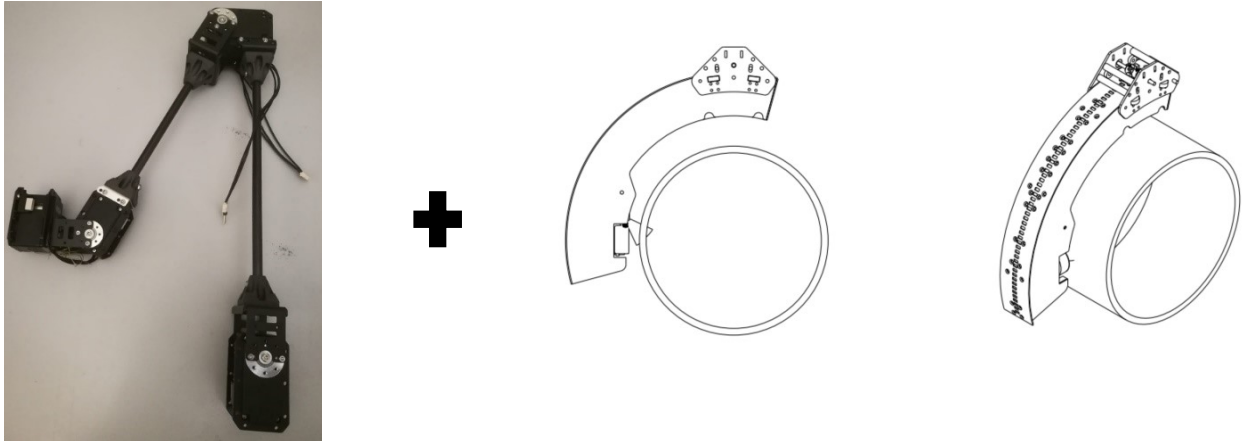


Figure 70 ARAP90 design

Tech specs:

- Arm weight 830g
- Tool weight 300g
- Arm payload: 670g
- Permitted tool rotation: 90 degrees
- Number of UT sensors: 1
- Number of DoFs: 6+1

3.6.4. Snake Arm with pan and tilt Probe (SAP)

The SAP is the most complex solution we designed with a target TRL 3. In detail, this prototype has been designed to further improve the dexterity and flexibility of previous systems, i.e., to work in a wide range of scenarios. In particular, the SAP is composed of:

1. A pan and tilt motor box connecting the arm with the drone frame.
2. A hyper-redundant robotic snake arm.
3. A pan and tilt probe with a single UT sensor.

Tech specs:

- Arm weight 2400g
- Tool weight 530g
- Arm payload: 300g
- Number of UT sensors: 1
- Number of actuated DoFs: 12
- Number of Joints: 21 (2 m.box, 1 pan-tilt, 18 snake)

In Figure 71 and Figure 72, the SAP is shown in different configurations to demonstrate its flexibility. The folded configuration on the top of the drone frame is also shown.



Figure 71 SAP design and proof of concept

In the following figure, the main dimensions of the SAP are shown. This version has been designed for pipes up to 12 inches. However, thanks to the modular design, such a system can be scaled down or scaled up to match different pipe size.

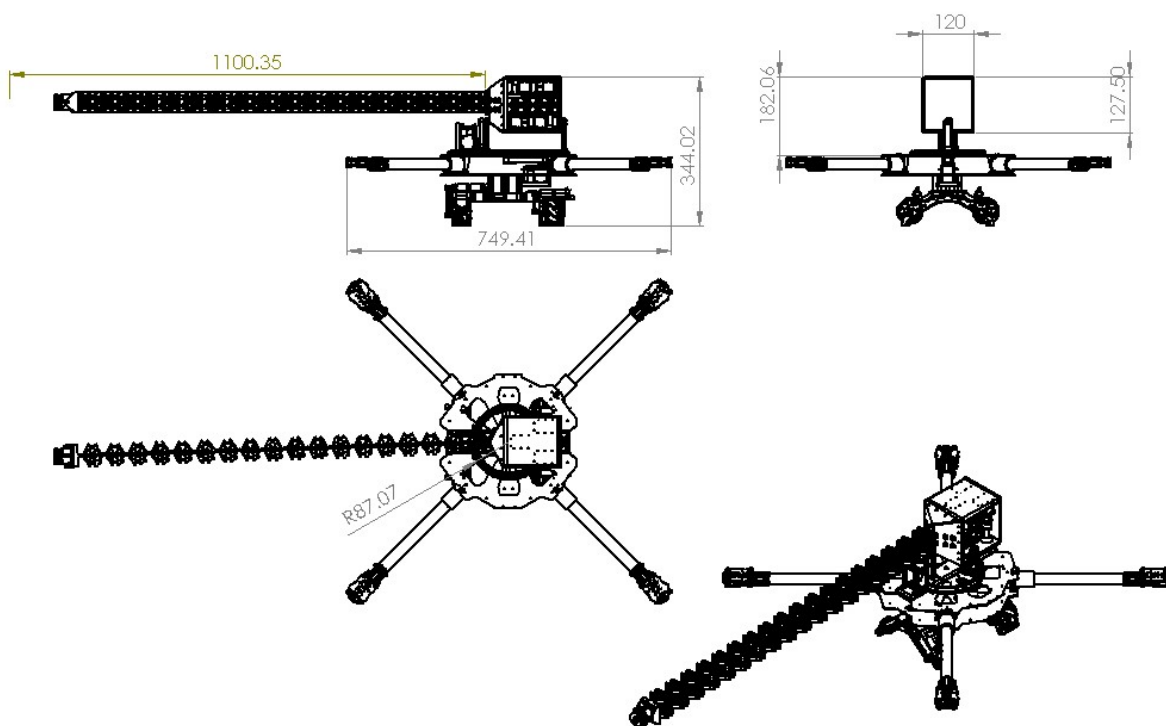


Figure 72 SAP dimensions

4. Coverage Analysis with Project Requirements

This section presents an analysis of the project requirements that were included in Deliverable D1.1, and the coverage of each of the relevant requirements by the HMR and HRA designs that are explained in this document. The analysis is presented in Table 11, where the requirement labels in the “ID” column correspond to the requirements defined in Table 3 of Deliverable D1.1. The corresponding cells in the HMR and HRA columns are coloured in green if the requirement is fulfilled, in yellow if it is only partially fulfilled or it needs more testing or development, and in red if it is not fulfilled in the actual design.

ID	Description	HMR	HRA
UR-01	System small enough to be transported by van or pallet	Complete system is small enough for transporting it by a car, indeed a person should be able to do it.	Complete system is small enough for transporting it by a car, indeed a person should be able to do it.
UR-02	System small enough to be transported by helicopter	Complete system is small enough for transporting it by a car, indeed a person should be able to do it.	Complete system is small enough for transporting it by a car, indeed a person should be able to do it.
UR-03	System small enough to be transported by airfreight cargo	Complete system is small enough for transporting it by a car, indeed a person should be able to do it.	Complete system is small enough for transporting it by a car, indeed a person should be able to do it.
UR-05	Gas detection system onboard the robotic vehicle	System will integrate a gas sensor	System will integrate a gas sensor
UR-07	Batteries protected against impacts	Protection mechanism has to be designed. Work has not started yet.	Protection mechanism has to be designed. Work has not started yet.
UR-08	Maximum weight of transporting box 30Kg	Transporting box will weigh less than 30 Kg. Box has not been designed yet.	Transporting box will weigh less than 30 Kg. Box has not been designed yet.
UR-13	Only brushless motors can be used	Brushless motors currently integrated.	Brushless motors currently integrated.

UR-14	Robotic vehicle has to be collision-proof (for example mechanical protection around propellers)	Propellers have been protected against collisions.	Propellers have been protected against collisions.
UR-16	Confirm clear areas for landing on top of pipes	HMR will send video information to the operator and it will be able to obtaining additional information from the integrated sensors (point cloud, depth images, etc.)	HRA will send video information to the operator and it will be able to obtaining additional information from the integrated sensors
UR-17	Pipe diameter from 8 to 20 inches (nominal)	HMR will be able of landing on pipes between 8 to 20 inches	HRA will be able of landing on pipes between 6 to 20 inches
UR-18	Pipes with 6 inches (nominal) diameter	HMR is expected to be able to land on pipes of 6 inches. Satellite designed to only cover down to 8 inches.	HRA will be able of landing on pipes of 6 inches
UR-19	Pipe diameter from 20 to 24 inches	HMR will be able of landing on pipes between 8 to 20 inches	HRA is not expected to land on pipes larger than 20 inches
UR-20	Magnetic pipes	HMR will be able of landing on magnetic pipes	HRA will be able of landing on magnetic pipes
UR-21	Non-insulated pipes	HMR will be able to land only on magnetic non-insulated pipes	HRA will be able of landing on non-insulated pipes
UR-25	The robotic system should be able to cross 5mm high welds	System has been designed for being able to cross 5mm high welds. Pending tests	System has been designed for being able to cross 5mm high welds. Pending tests
UR-26	The robotic system should be able to cross horizontal elbows	System has been designed for being able to cross horizontal elbows. Pending tests	System can cross horizontal elbows.

UR-27	Robotic system able to move along the pipe	HMR can move along the pipe.	HRA can move along the pipe.
UR-28	It is needed to assess the surface condition of top of the pipe	The system will incorporate the sensors that allow the pilot to assess the condition of the pipe. In this case, the HMR will have integrated several cameras.	The system will incorporate the sensors that allow the pilot to assess the condition of the pipe. In this case, the HRA will have integrated several cameras.
UR-29	Assess surface condition 360° around the pipe	The HMR will have integrated several cameras. For knowing if it is able to covering 360° it is necessary to perform some tests.	The HRA will have integrated several cameras. For knowing if it is able to covering 360° it is necessary to perform some tests.
UR-30	Locate the weld	The system will incorporate cameras that allow the pilot to locate welds in real time.	The system will incorporate cameras that allow the pilot to locate welds in real time.
UR-31	Accuracy location at 1 cm level to the weld and with respect to 3, 6, 9 and 12 positions	The satellite can follow an inspection path within 1 cm relative accuracy. Absolute accuracy within the capability of visual reference via HD FPV camera. Visual accuracy subject to testing.	System has been designed for being able to localize itself with a relative accuracy of 1cm with respect to welding section. Pending tests
UR-32	Accuracy location at 2 cm level to the weld and with respect to 3, 6, 9 and 12 positions	The satellite can follow an inspection path within 2 cm relative accuracy. Absolute accuracy within the capability of visual reference via HD FPV camera. Visual accuracy subject to testing.	System has been designed for being able to localize itself with a relative accuracy of 1cm with respect to welding section. Pending tests
UR-34	Be able to save and display in real-time A-SCAN data from the ground	Ultrasonic HMI allows displaying and recording SCAN data from the ground	Ultrasonic HMI allows displaying and recording SCAN data from the ground

UR-35	Be able to control de ultrasonic sensor from the ground	Ultrasonic HMI allows controlling the ultrasonic sensor from the ground	Ultrasonic HMI allows controlling the ultrasonic sensor from the ground
UR-36	Pipe temperature will be less than 60°C	To be tested	To be tested
UR-37	Pipe temperature can be as high as 100°C	To be tested	To be tested
UR-38	Robotic system MTOW less than 8kg	HMR has been designed to weigh less than 8 kg.	At first instance, HRA has been designed to weigh less than 15 kg. However, probably it will weigh less than 8 kg.
UR-39	Robotic system MTOW less than 15kg	HMR has been designed to weigh less than 8 kg.	HRA has been designed to weigh less than 15 kg.
UR-41	Quadrant horizontal elbow inspection: 4 points (3, 6, 9 and 12 positions) close to first weld, 4 points close in the middle and 4 points close to second weld	The satellite of the HMR will be able to perform ultrasonic inspection at 3, 6, 9 and 12 positions in the first, middle and second welds	The arm of the HRA will be able to perform ultrasonic inspection at 3, 6, 9 and 12 positions in the first, middle and second welds
UR-42	Quadrant vertical elbow inspection: 4 points (3, 6, 9 and 12 positions) close to first weld, 4 points in the middle and 4 points close to second weld	The HMR satellite will be able to perform ultrasonic inspection at 3, 6, 9 and 12 positions in the first, middle and second welds	The HRA arm will be able to perform ultrasonic inspection at 3, 6, 9 and 12 positions in the first, middle and second welds
UR-43	Grid inspection on elbows	The satellite will be able to perform grid inspections on elbows with stitched line scans in longitudinal directions.	The HRA arm will be able to perform grid inspection on elbows
UR-44	Grid inspections on horizontal T joint inspection in 1 and 3	The satellite will be able to perform grid inspections on T joints in areas where surface curvature is larger than	The HRA arm will be able to perform grid inspection on elbows

	areas (including impact area)	D8". Subject to further testing.	
UR-45	Horizontal quadrant T joint inspection in 1 and 3 areas (including impact area)	The satellite will be able to perform horizontal quadrant T joint inspection in 1 and 3 areas (including impact area) in areas where surface curvature is larger than D8". Subject to further testing.	The HRA-SAP arm will be able to perform horizontal quadrant T joint inspection in 1 and 3 areas (including impact area)
UR-46	Grid inspection on reducers and T joint in area 2	The satellite will be able to perform grid inspections on reducers and T joint in area 2 in areas where surface curvature is larger than D8". Subject to further testing.	The HRA-SAP arm will be able to perform grid inspection on reducers and T joint in area 2
UR-47	Reducers and T joint in 2 quadrant inspections	The satellite will be able to perform 2 quadrant inspections on reducers and T-joints.	The HRA-SAP arm will be able to perform reducers and T joint in 2 quadrant inspections
UR-48	Horizontal pipe quadrant inspection until first weld whatever the configuration	The HMR will be able to perform pipe quadrant inspection until the first weld whatever the configuration.	The HRA arm will be able to perform horizontal pipe quadrant inspection until first weld whatever the configuration
UR-49	minimum pipe-to-pipe distance 75mm	The satellite has been designed for a minimum distance between pipes of 100 mm	HRA is able of inspecting pipes with a separation of 75mm
UR-50	Take into consideration pipes that are close to each other	HMR is able to take off from a pipe and go to another.	HRA is able to perform an inspection in a close pipe.

UR-57	Be able to change or recharge batteries onsite (in safe areas only)	Batteries can be charged in anywhere	Batteries can be charged in anywhere
UR-58	Be able to reload ultrasonic coupling onsite (if applicable)	Ultrasonic coupling can be reloaded easily onsite	Ultrasonic coupling can be reloaded easily onsite

Table 11: Requirements coverage

5. Conclusions

This document has presented the design of the HYFLIERS hybrid robot prototypes, the HMR and the HRA. The design is based on the initial system specifications in Deliverable D1.1 the system concept architecture in Deliverable D1.2. The deliverable presents the detailed design of the HMR including the aerial platform and the satellite, and the HRA, including the aerial platform with the landing modules and the arm.

One of the main drivers of the presented designs is the large variability of operational cases that appear in pipe inspection in an oil&gas plant, as highlighted by the end users. In a refinery there are thousands of kilometres of pipes that have to be inspected, which from the simplest case of a straight, isolated pipe, they can have diameters from 6 to 24 inches, have horizontal or vertical elbows, T's, reductions, be made of magnetic/non-magnetic material, be in racks with different separations between them (or no separation), be at different heights in the rack with/without access from the top, need inspection in one point/several points/area, etc. The HYFLIERS hybrid robot designs with two different prototypes with a satellite robot and an arm, and the modular configuration tries to cover as much as possible the different operational cases that will arise in pipe inspection.

These designs need extensive development, integration and testing in the lab and in the refinery to refine the designs and validate the range of cases in which they will be able to operate.

References

- [1] HYFLIERS Deliverable D1.1 “Initial System Specification”, March 2018.
- [2] HYFLIERS Deliverable D1.2 “System Concept and Architecture”, June 2018.
- [3] Ramon-Soria, P., A.E. Gomez-Tamm, F.J. Garcia-Rubiales, B.C. Arrue, and A. Ollero. “Autonomous landing on pipes using soft gripper for inspection and maintenance in outdoor environments”. In 2019 IEEE/RSJ International Conference on Intelligent Robots and Systems (IROS), Macao, Nov. 2019 (accepted for publication).
- [4] Zhang, X., X. Zhou, M. Lin and J. Sun, “ShuffleNet: An Extremely Efficient Convolutional Neural Network for Mobile Devices”. 2018 IEEE/CVF Conference on Computer Vision and Pattern Recognition (CVPR), 2018.
- [5] Cutler, M., N.-K. Ure, B. Michini, and J. How, "Comparison of fixed and variable pitch actuators for agile quadrotors," in AIAA Guidance, Navigation, and Control Conference, 2011, pp. 6406-6423.
- [6] Cutler, M.J., "Design and control of an autonomous variable-pitch quadrotor helicopter." 2012, Doctoral dissertation, Massachusetts Institute of Technology, Department of Aeronautics and Astronautics, Citeseer.
- [7] Nekoo, S.R., J.A. Acosta and A. Ollero. “Fully Coupled Six-DoF Nonlinear Suboptimal Control of a Quadrotor: Variable-pitch Rotor Design”. ROBOT 2019 Iberian Robotics Conference, Porto, Portugal, Nov. 2019 (submitted).
- [8] Bhargavapuri, M., S.R. Sahoo, and M. Kothari, "Robust nonlinear control of a variable-pitch quadrotor with the flip maneuver," Control Engineering Practice, 87, pp. 26-42, 2019.
- [9] HYFLIERS Deliverable D3.1 “Lightweight hyper-redundant robotic arm for aerial inspection tasks”, June 2019.